MURILO COSTA CAMPOS DE MOURA

STOCHASTIC MODELING OF THE LEVELIZED COST OF HYDROGEN PRODUCED VIA AMMONIA ELECTROLYSIS

São Paulo
2024

MURILO COSTA CAMPOS DE MOURA

STOCHASTIC MODELING OF THE LEVELIZED COST OF HYDROGEN PRODUCED VIA AMMONIA ELECTROLYSIS

Graduation Work presented to the Escola Politécnica – University of São Paulo for attaining the Bachelor's Degree in Production Engineering.

Advisor: Prof. Dr. Celma de Oliveira Ribeiro

São Paulo
2024

To Mari and Marquinho

ACKNOWLEDGMENTS

I would like to express my heartfelt gratitude to the teachers and staff at Escola Politécnica, in particular to my advisor Prof. Celma Ribeiro, who contributed greatly with their knowledge and provided me with a role model for my professional activity.

I would also like to thank my friends from Não Vai, CAEP and G20 who accompanied me through this journey. A special mention to Isadora Wistrøm for her love and support, specially in this last chapter.

Finally, I am deeply grateful to my family members. My heartfelt appreciation goes out to my sister, Luísa, my brother-in-law Marcos, as well as to my parents, José Euclides and Vera Simone. Your support has pushed me to go further. I also extend my gratitude to my dear grandmothers, Conceição and Gladys, as well as my aunts, uncles and cousins who rooted for me during my studies.

"Quem quer passar além do Bojador
Tem que passar além da dor."

– Fernando Pessoa

ABSTRACT

The growing urgency to decarbonize the global economy has placed hydrogen at the forefront of sustainable energy solutions. Among hydrogen production methods, ammonia electrolysis offers significant potential by utilizing existing ammonia infrastructure and supply chains. This study employs stochastic modeling to estimate the Levelized Cost of Hydrogen (LCOH) for ammonia electrolysis, comparing it with the more established water electrolysis process. The analysis integrates uncertainty in critical parameters, such as electricity costs, capacity factors, and equipment refurbishment events, using Monte Carlo simulations combined with the ProFAST Python library. Key scenarios for electricity sourcing, including grid and wind-based power, are evaluated to assess the influence of energy supply variability on cost dynamics. The study identifies the primary cost drivers and evaluates the feasibility of ammonia electrolysis as a competitive option for green hydrogen production, offering strategic insights to support the transition to a low-carbon energy economy.

Keywords – Hydrogen, Ammonia, Electrolysis, Monte Carlo simulation, Stochastic modeling, Levelized Cost of Hydrogen (LCOH).

LIST OF FIGURES

LIST OF TABLES

CONTENTS

1 INTRODUCTION

The global climate crisis has reached unprecedented levels, with data indicating an accelerating trajectory of environmental degradation. According to recent data from the International Energy Agency (IEA), energy-related CO2 emissions achieved a historic peak of 37.7 gigatonnes (Gt) in 2023, marking a 1.3% increase from the previous year (IEA, 2024c). This concerning trend is predominantly driven by the energy sector, which accounts for approximately 85% of global CO2 emissions, with coal consumption being the primary contributor to the recent surge.

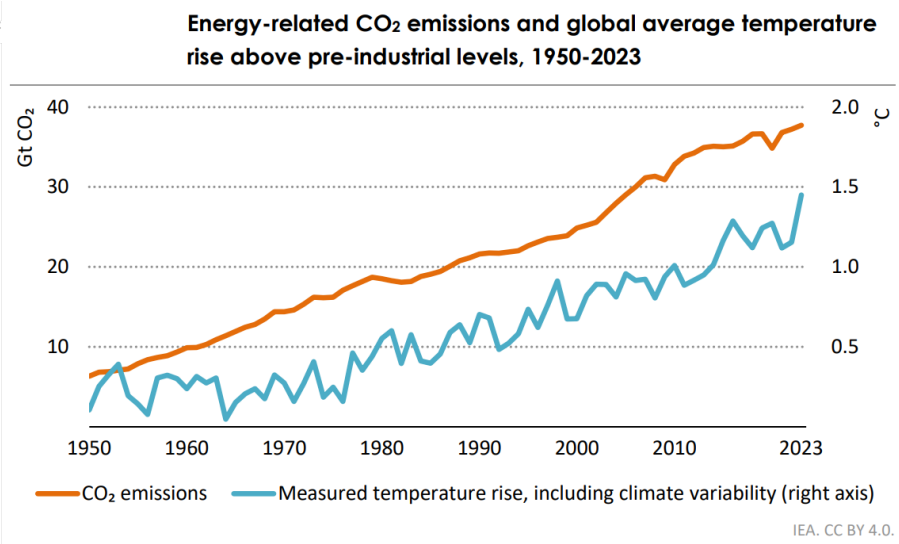

Figure 1: Energy-related CO2 emissions and global average temperature rise above pre-industrial levels

Source: (IEA, 2024c)

The severity of this crisis is further exemplified by recent temperature records. The year 2023 was registered as the warmest in recorded history, with early indicators suggesting that this record may be surpassed in 2024. In the twelve months leading to May 2024, 76 extreme heat events were documented worldwide, resulting in substantial disruptions to infrastructure, healthcare services, and vulnerable populations (CLIMATE CENTRAL, 2024).

Average global surface temperatures during this same period suggest the world is nearing the critical threshold of 1.5°C above pre-industrial levels (C3S, 2024). Although the Paris Agreement aims to maintain long-term warming below 1.5°C, short-term exceedances highlight the fragility of this target. Without immediate and sustained global action, the consequences of surpassing this threshold could be catastrophic, as emphasized by the Intergovernmental Panel on Climate Change (IPCC, 2023).

The imperative to decarbonize the global economy has never been more urgent. Despite the expanding deployment of clean energy technologies, which has helped curtail emissions growth by two-thirds compared to business-as-usual scenarios (IEA, 2024a), more transformative solutions are still required. In this context, green hydrogen has emerged as a critical enabler of deep decarbonization, with applications spanning industrial processes, transportation, and energy storage, offering a versatile pathway toward achieving carbon neutrality.

Among the various methods for green hydrogen production, ammonia electrolysis presents a particularly promising avenue. This process not only enables the production of clean hydrogen but also leverages existing ammonia infrastructure and transportation networks, potentially lowering the overall costs and logistical challenges of hydrogen deployment. Assessing the economic feasibility of ammonia electrolysis is therefore essential for guiding strategic decisions and policy development in the global shift toward a low-carbon economy.

This study aims to develop a comprehensive stochastic model to estimate the Levelized Cost of Hydrogen (LCOH), incorporating the simulation of equipment failures throughout the plant's lifecycle. The analysis will compare the performance and cost dynamics of ammonia electrolysis with the more established water electrolysis process. Additionally, the study will identify the primary cost drivers for each method, providing valuable insights to inform the development and optimization of green hydrogen technologies.

2 LITERATURE REVIEW

2.1 Energy transition

In light of the serious risks to the planet associated with human-induced climate change, largely stemming from fossil fuel use, there is growing consensus that a transition in energy production and consumption is essential (York; Bell, 2019).

Central to the energy transition is the decarbonization of electricity generation and fuels, which necessitates a substantial reduction in carbon intensity and a comprehensive shift toward low-carbon energy sources. In scenarios that avoid overshooting the 1.5°C target by 2050, renewables are expected to account for 52% to 67% of primary energy supply , while coal use is projected to fall drastically, generally limited to cases where it is coupled with carbon capture and storage (CCS) technologies (see figure 2). This shift is complemented by a sharp increase in electrification across the transportation and industrial sectors, raising electricity's share of final energy consumption to an estimated 34% to 71% by mid-century. Moreover, significant energy demand reductions across sectors are projected, driven by efficiency improvements and shifts in consumption patterns. (IPCC, 2018)

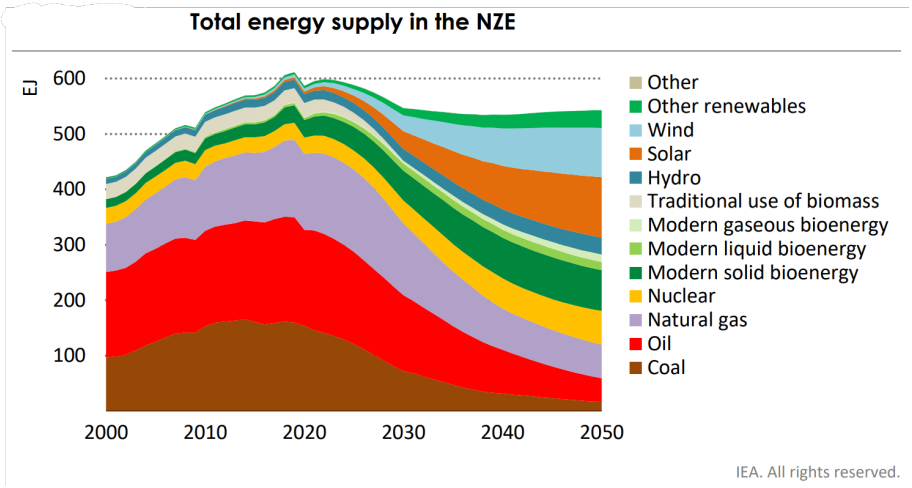

Figure 2: Evolution of the energy mix towards a net-zero scenario in 2050
Source: (IEA, 2021)

However, at present, the transition is taking place at a slower pace than required. Demand for energy is still growing globally, driven by economic growth and population increases. This escalating demand poses a dual challenge: new low-carbon energy sources must not only fulfill additional consumption needs but also replace fossil fuels in the current energy mix to reduce carbon emissions effectively (Ritchie; Rosado; Roser, 2020).

Recent data underscores the urgency of this challenge. In 2022, global energy demand surged by 8 exajoules (EJ), followed by an even larger increase of approximately 13 EJ in 2023 (see figure 3). This 2% rise in global demand reflects a significant energy requirement in emerging and developing economies, which more than offset a 2% decline in energy demand within advanced economies. The increased demand was primarily met by fossil fuels, with oil and coal consumption seeing notable rises. In fact, fossil fuels accounted for two-thirds of the total energy demand increase in 2023 (IEA, 2024c).

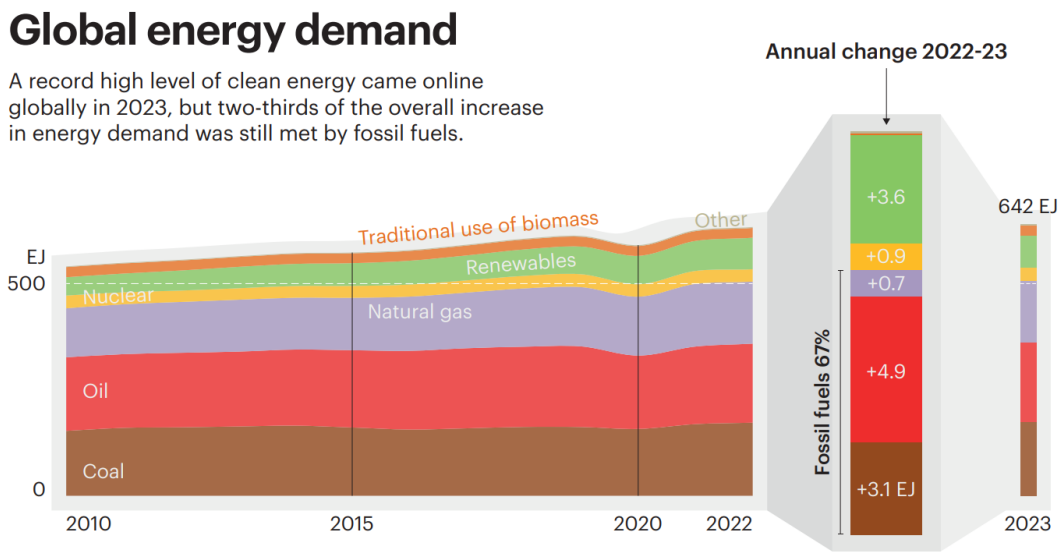

Figure 3: Energy demand increase in 2023
Source: (IEA, 2024c)

Smil (2019) highlights historical patterns that reveal a slow and incomplete transition from traditional biofuels to modern energy sources over centuries. Despite advancements over the last two centuries, biomass fuels still contribute a small but persistent share of global energy. Similarly, coal, though its share has diminished as hydrocarbons like oil and gas gained prominence, still supplies a substantial portion of energy (see figure 4). Crude oil, despite some countries reducing their dependency following the 1970s price shocks, remains the primary global energy source, underscoring the enduring dominance of fossil fuels in the energy landscape and suggesting that the current energy transition will also be prolonged.

York and Bell (2019) observe that this pattern reflects a broader issue of structural inertia

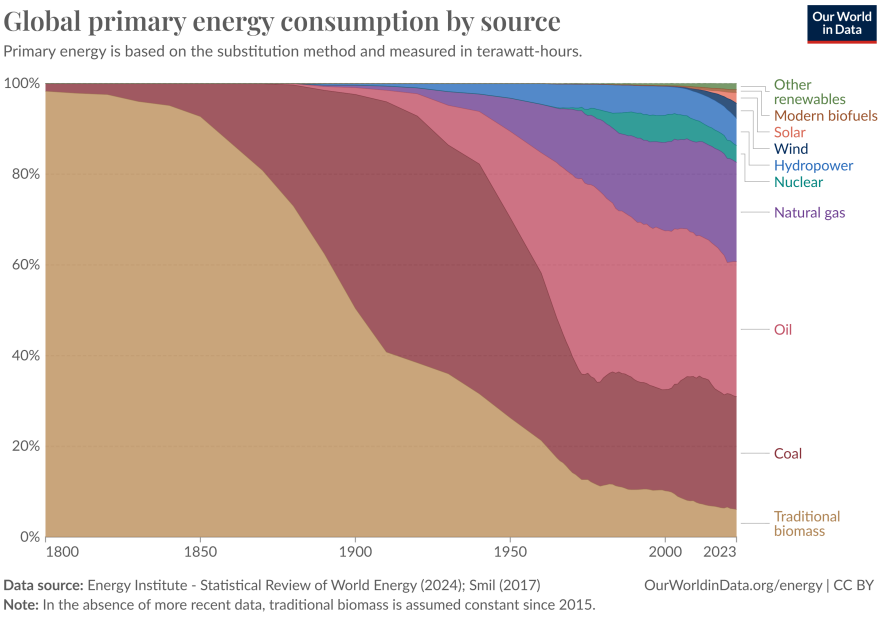

Figure 4: Evolution of the share of primary energy sources
Source: (Ritchie; Rosado; Roser, 2020)

within energy systems, where the incumbent fossil fuel regime continues to benefit from existing infrastructure, market dominance, and policy support. The result is a system in which renewables expand without necessarily reducing fossil fuel use significantly, posing the risk of continuing the cycle of energy additions rather than achieving the carbon reduction needed for climate goals. The authors highlight that this "addition" phenomenon not only fails to displace fossil fuel use but could, all else equal, reinforce it by lowering overall energy prices, thus stimulating further consumption.

The scale and scope of a true energy transition, as Davidson (2019) asserts, will require a systematic approach involving both innovation in renewable technologies and deliberate action to phase out fossil fuels. According to the author, governments and institutions must consider policies that actively limit fossil fuel extraction and consumption, potentially through carbon pricing, regulatory frameworks, and fossil fuel divestment initiatives. Additionally, Fouquet (2016) notes that policy and government intervention have historically played crucial roles in energy transitions, indicating that achieving a contemporary transition to renewables will likely depend on similar levels of governmental action to create conducive environments for renewable adoption and fossil fuel decline.

2.2 Hydrogen

Hydrogen is expected to play a pivotal role in the ongoing energy transition, providing a versatile, carbon-neutral energy carrier that addresses hard-to-abate sectors where renewable electricity alone may be insufficient. In particular, hydrogen can support long-distance heavy transport and industrial processes demanding high-temperature heat, such as those in the steel and cement industry. Moreover, hydrogen's ability to store energy over long durations and convert it back to power when needed also makes it valuable for mitigating the intermittency issues of renewable energy sources like wind and solar (Oliveira; Beswick; Yan, 2021).

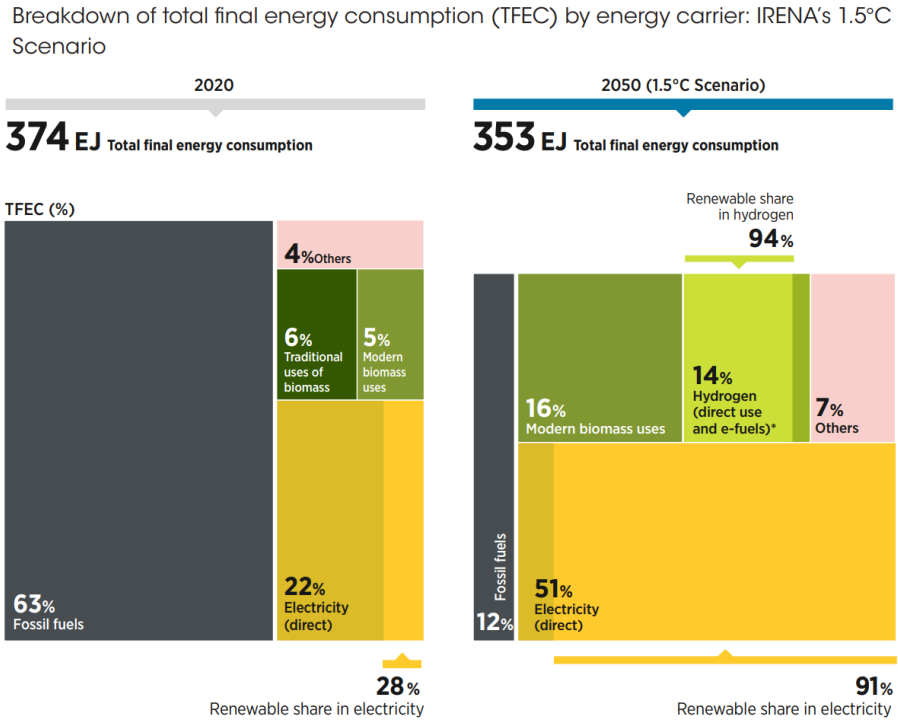

Figure 5: Projected share of energy carriers in a net-zero scenario
Source: (IRENA, 2024)

In a net-zero until 2050 scenario, hydrogen is projected to account for 14% of the total final energy consumption, driven mostly by hard to electrify uses (see figure 5). This means production would need to increase by over five times from current numbers to meet the future demand (IRENA, 2024).

2.2.1 The "colors" of hydrogen

Hydrogen is not all produced equally, and its sustainability depend largely on the emissions intensity associated with its production process. To distinguish between varying environmental impacts, hydrogen is often categorized by color, each indicating the carbon intensity of its pro-

duction. Several different classifications exist, so in table 1 are presented those most commonly found in the literature (Incer-Valverde et al., 2023).

	Gray hydrogen	Blue hydrogen	Green hydrogen
Process	Reforming or gasification	Reforming or gasification with carbon capture	Electrolysis
Energy source	Fossil fuels	Fossil fuels	Renewable energy

Table 1: Hydrogen production pathways
Source: (IRENA, 2024)

Gray hydrogen is produced from fossil fuels, such as natural gas or coal, without implementing carbon capture and storage (CCS) technologies, leading to substantial CO_2 emissions. The global production of hydrogen, which amounted to around 97 million tonnes in 2023, relies today almost exclusively on gray hydrogen, with around two thirds of this amount coming from natural gas reforming (IEA, 2024b).

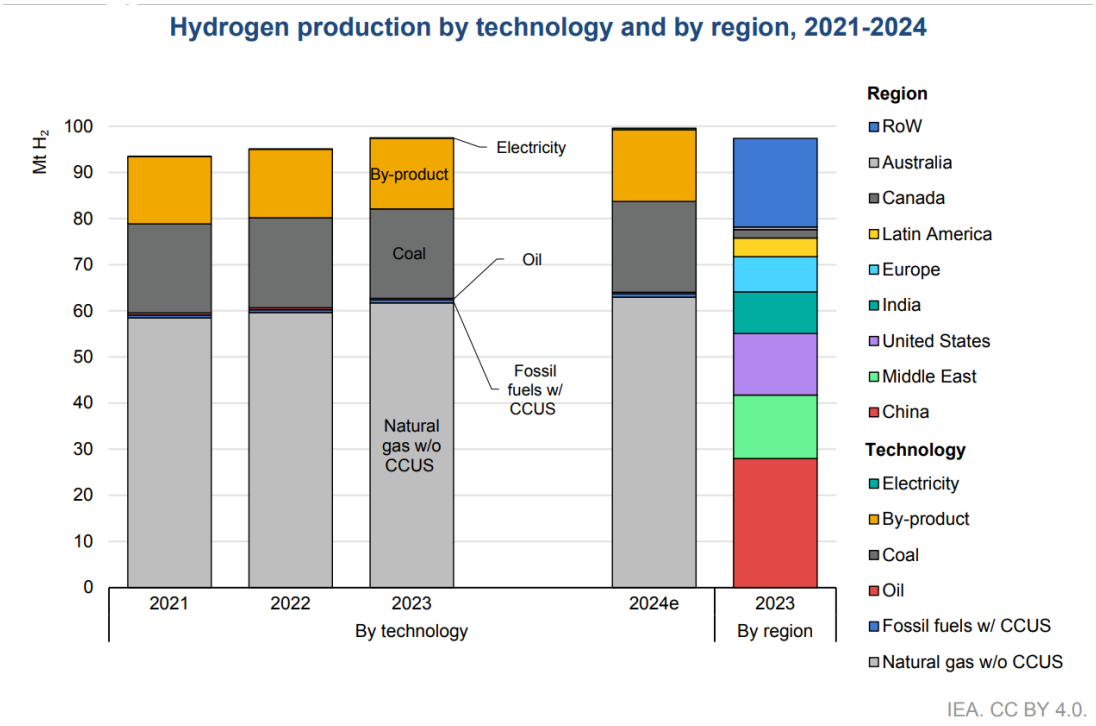

Figure 6: Hydrogen production by technology and by region
Source: (IEA, 2024b)

Blue hydrogen involves the same production process as gray hydrogen, primarily steam methane reforming of natural gas, but incorporates carbon capture and storage (CCS) technologies to trap and sequester the carbon dioxide emissions. According to the IEA (2024b), it is currently the main source of low emisison hydrogen, but still corresponds to less then 1% of total hydrogen production in 2023. Blue hydrogen is viewed by some as a pragmatic and cost-

effective bridge towards a hydrogen economy since it can be produced from the retrofitting of the already existing gray hydrogen infrastructure (Ehlig-Economides; Hatzignatiou, 2021).

Nonetheless, this view has found growing opposition in academia. Howarth and Jacobson (2021) argue that the lifecycle emissions of blue hydrogen, which include fugitive methane leaks and residual carbon dioxide, are only marginally lower than those of gray hydrogen. Methane has a much greater short-term warming effect compared to carbon dioxide, exacerbating blue hydrogen's environmental impact. Specifically, the total CO_2 equivalent emissions for blue hydrogen are found to be only 9-12% lower than gray hydrogen, and, in fact, 20% higher than direct natural gas or coal combustion for heat, which would make its use as an emissions reduction measure a nonsense. The authors also underscore that their analysis assumes that captured CO_2 can be stored indefinitely, which is an optimistic best-case assumption.

Green hydrogen, produced by electrolysis using renewable electricity from sources such as wind or solar energy, is expected to be a pivotal element in the transition to a fully renewable energy society. Unlike gray or blue hydrogen, green hydrogen is associated with zero direct emissions, making it a highly attractive option for decarbonizing various sectors (Kovač; Paranos; Marciuš, 2021).

The European Union (EU) has defined its own criteria to classify green hydrogen, stipulating that it must be produced in countries where over 90% of the electricity comes from renewable energy sources (RES) or where the emissions intensity of the electricity used falls below a specified threshold (EUROPEAN COMISSION, 2023). One of the primary principles in EU's framework is "additionality," which requires hydrogen electrolysers to be connected to newly generated renewable electricity sources, thereby ensuring that green hydrogen production does not strain existing renewable supplies but instead promotes an overall increase in renewable energy generation. Moreover, the framework introduces criteria for "temporal and geographic correlation" to ensure hydrogen is produced when and where renewable energy is available, helping to align production with decarbonization goals and avoid undue pressure on the power grid (EUROPEAN COMISSION, 2023).

However, green hydrogen still remains a very small fraction of total hydrogen production, with less than 100 kilotons (kt) produced globally in 2023. This limited production is concentrated mainly in China, Europe, and the United States, which together account for approximately 75% of global electrolytic hydrogen output. Despite its immense potential, the scalability of green hydrogen production remains a significant hurdle, largely due to high production costs and the need for advancements in electrolysis technologies such as Proton Exchange Membrane (PEM) and Alkaline (ALK) (IEA, 2024b). These and other challenges will be further

discussed in section 2.2.3.

2.2.2 Current and projected future applications of Hydrogen

This section examines hydrogen's current applications and anticipated future roles using the framework delineated by Oliveira, Beswick and Yan (2021), who envisions a phased approach (see figure 7) to ramp up hydrogen's demand and integrate it across sectors to meet diverse energy needs while reducing greenhouse gas emissions.

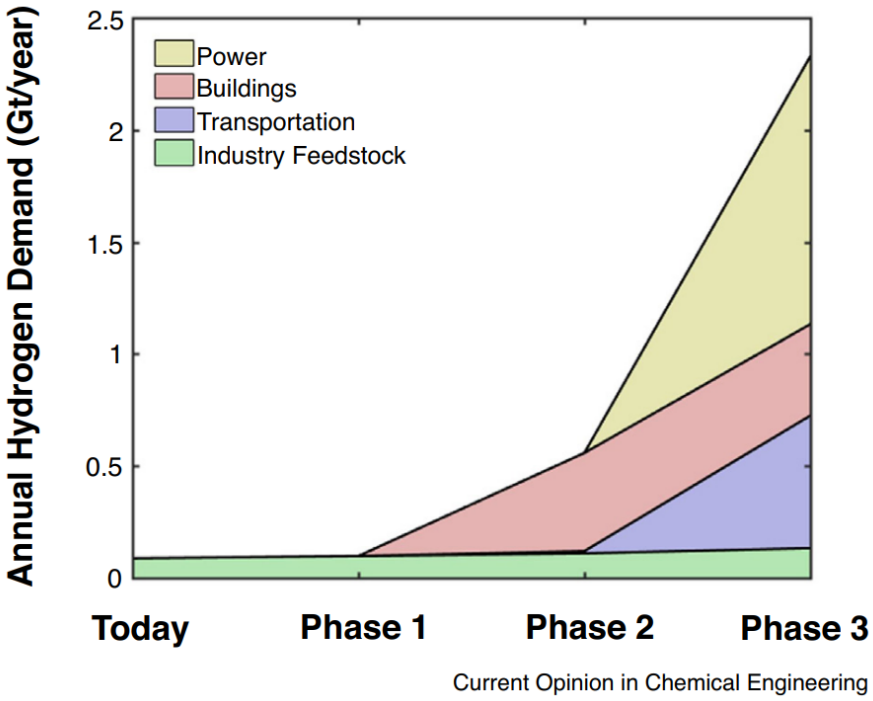

Figure 7: Ramp-up phases of hydrogen demand
Source: (Oliveira; Beswick; Yan, 2021)

Phase 1: Hydrogen as an industrial feedstock

In the first phase of the framework developed by Oliveira, Beswick and Yan (2021), green hydrogen will be employed as the main route to decarbonize industrial processes which are currently reliant on gray hydrogen. Kovač, Paranos and Marciuš (2021) note that ammonia synthesis alone constitutes 55% of the current global demand for hydrogen, while oil refining represents 25%, and methanol synthesis accounts for 10%.

Hydrogen feedstock could also penetrate other CO_2 intensive chemical synthesis processes. The steel manufacturing process, which is one of the largest carbon emitters globally, accounting for nearly 6% of all emission, could be transformed through direct reduced iron (DRI) processes that use hydrogen (IRENA, 2018).

Phase 2: Fuel for transportation and heat

In the second phase, green hydrogen begins to be introduced in sectors beyond chemical synthesis, particularly transportation and heating (Oliveira; Beswick; Yan, 2021).

In heavy-duty and long-range transportation applications, battery electric vehicles (BEVs) face limitations due to battery weight and prolonged charging times, which undermine their practicality for such uses. Hydrogen fuel cell electric vehicles (FCEVs) emerge as a promising alternative in this context. Owing to hydrogen's higher energy density and shorter refueling times, FCEVs offer competitive advantages for long-haul freight trucks, buses, and other commercial vehicles (Cano et al., 2018).

While some industrial processes, like steelmaking discussed in Phase 1, may transition to electrochemical methods, thermal processes requiring temperatures above 400ºC still necessitate high-grade heat sources. The combustion of pure hydrogen can provide the requisite heat, assuming that furnaces and boilers are retrofitted appropriately for hydrogen use (Oliveira; Beswick; Yan, 2021). For example, cement production contributes to approximately 7% of global CO_2 emissions, with 40% of these emissions stemming from the combustion of fuels needed to heat kilns to temperatures as high as 1450ºC (IEA et al., 2018).

Phase 3: Energy storage

The final phase of the framework envisions hydrogen as a seasonal energy storage medium and a key contributor to producing synthetic e-fuels for industries such as aviation and marine transport (Oliveira; Beswick; Yan, 2021).

Renewable sources like solar and wind are inherently intermittent, and hydrogen's role as a storage medium can help mitigate these fluctuations. While lithium-ion batteries can efficiently provide grid stability over hours, they are less feasible for multi-day or seasonal storage due to their self-discharge rates and high costs when scaled up (Kovač; Paranos; Marciuš, 2021). By contrast, hydrogen can store energy for months without significant loss, enabling grid operators to meet seasonal demands, especially in regions with extreme weather variations, therefore reducing curtailment and improving renewable utilization (Ma et al., 2024).

In addition to this application, Oliveira, Beswick and Yan (2021) highlight that electrification is not feasible for certain transportation sectors, notably aviation, where kerosene-based jet fuels are predominant. These fuels currently contribute 918 Mt of CO_2 emissions annually, a figure projected to escalate to 2.6 Gt by 2050 due to a 2.4% annual growth in air freight and a tripling of passenger aviation (U.S. Energy Information Administration, 2019; Graver; Zhang; Rutherford, 2019). The transition to green technologies in aviation is challenging because high

volumetric energy density and low weight are critical so batteries and fuel cells presently cannot meet the power demands of large, long-haul aircraft without adding prohibitive weight or requiring excessive storage space (Hall; Pavlenko; Lutsey, 2018).

However, hydrogen offers a possible alternative by being converted into e-fuels. One pathway involves the Fischer-Tropsch process, where hydrogen and carbon monoxide produced by converting captured CO_2 are synthesized into carbon-neutral synthetic jet and diesel fuels (König et al., 2015). In the marine industry, e-fuels have also been proposed to decarbonize larger freight ships, while smaller passenger vessels might adopt fuel cells to replace traditional fuels and diesel generators (Oliveira; Beswick; Yan, 2021).

2.2.3 Challenges to the hydrogen economy

Hydrogen offers significant potential for decarbonizing various sectors, particularly those lacking viable electrification alternatives. However, considerable barriers hinder its widespread adoption (Rasul et al., 2022).

2.2.3.1 Production costs

One primary challenge in the hydrogen economy is the high cost of hydrogen production, particularly for green hydrogen. According to Agyekum et al. (2022), the production cost of green hydrogen currently ranges between $4-7 per kilogram, 2 to 3 times higher than hydrogen derived from fossil fuels. Kayfeci, Keçebaş and Bayat (2019) emphasize that the main drivers of these costs currently are electricity consumption and the need for improved efficiency and durable catalysts in the electrolysis process. This fact motivates further studies on how to make investing in those projects more appealing, so that economies of scale can bring costs down.

2.2.3.2 Storage and transportation challenges

Hydrogen storage poses another challenge due to its low volumetric energy density (see figure 8). Consequently, gaseous hydrogen must be stored at high pressures (up to 700 bar) or as a cryogenic liquid at -253°C to attain sufficient energy density for transportation and stationary energy storage applications (Cavaliere, 2023). Melaina, Antonia and Penev (2013) discuss hydrogen's high diffusivity, which results in losses of mass, and the necessity for materials that can prevent leakage and resist embrittlement, which occurs when hydrogen permeates materials, causing them to become fragile and prone to failure. This requires either costly retrofitting with advanced materials that resist hydrogen-induced damage or the development of entirely new

pipeline networks.

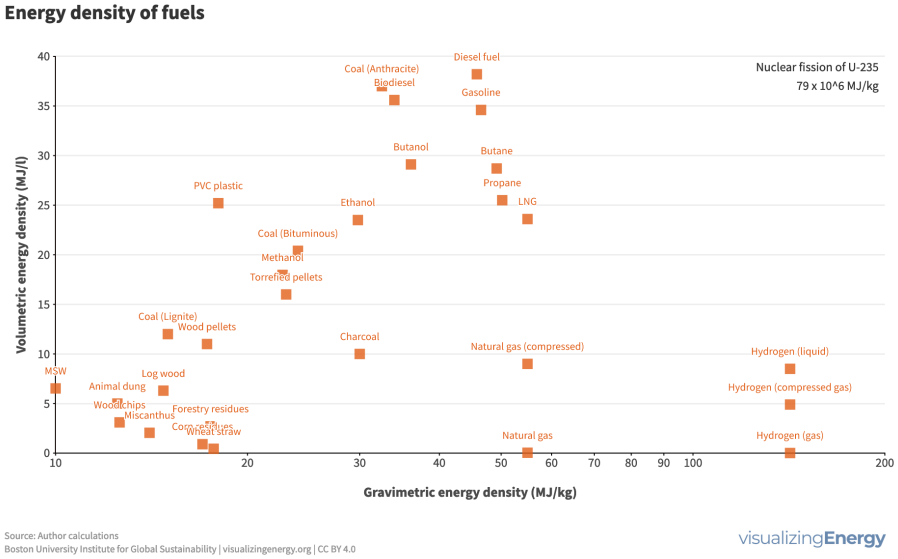

Figure 8: Energy density of different energy sources
Source: (Cleveland, 2024a)

Chemical carriers, such as ammonia and methanol, offer a means of storing hydrogen in a more stable form, potentially circumventing some safety and infrastructure challenges associated with pure hydrogen gas (Zamfirescu; Dincer, 2008). Ammonia, for instance, can be stored as a liquid at conditions similar to the ubiquitous propane gas (8 bar pressure and room temperature), releasing hydrogen upon decomposition with the aid of catalysts (Bell; Torrente-Murciano, 2016). According to Gonzalez-Garay et al. (2022), ammonia can be transported using existing infrastructure in the chemical industry, providing a potential pathway for hydrogen distribution without constructing a hydrogen-specific network. However, as Agyekum et al. (2022) note, these conversion processes introduce additional costs and energy losses, as hydrogen must be extracted from ammonia or methanol upon reaching its destination. The role ammonia can play in the hydrogen economy will be further discussed in section 2.3.

2.2.3.3 Environmental and safety concerns

The environmental impact and safety profile of hydrogen pose additional challenges. Squadrito, Maggio and Nicita (2023) highlight the substantial water requirements for hydrogen production via electrolysis, raising concerns about resource sustainability in water-stressed regions which otherwise have hight availability of renewables. Safety issues are equally complex. Melaina, Antonia and Penev (2013) note that hydrogen's flammability and explosive potential are intrinsic risks that necessitate rigorous safety standards. This is worsened by the fact that odorization, a standard method for identifying natural gas leaks, is less feasible with hydrogen. The odor-

ants would need to be sufficiently potent to alert personnel at a very low hydrogen concentration (20% of the lower flammability limit), but hydrogen's extreme purity requirements, especially for fuel cells and other high-efficiency applications, limit the use of such additives (Gerboni, 2016).

2.2.3.4 Policy and Regulatory barriers

The literature consistently highlights the role of policy in facilitating or hindering the adoption of hydrogen. According to Falcone, Hiete and Sapio (2021), one of the most pressing regulatory issues is the absence of standardized frameworks that support hydrogen production, distribution, and utilization across sectors. Currently, national and regional policies vary widely in their support for hydrogen, resulting in a fragmented regulatory landscape that complicates cross-border hydrogen trade and technology standardization. Standardization in hydrogen policies also addresses certification requirements, particularly regarding the "green" label for hydrogen produced with renewable energy. Certifying hydrogen as "green" requires rigorous verification processes, which are presently underdeveloped and vary across jurisdictions. As noted by Farrell (2023), this lack of unified certification standards can inhibit the market expansion of green hydrogen, as industries may lack confidence in the environmental credentials of hydrogen imported from different regions.

Another critical barrier is the lack of established markets for green hydrogen, especially in end-use sectors such as transportation. Unlike electricity, where market dynamics are well-established, hydrogen lacks a mature demand structure. As pointed out by Falcone, Hiete and Sapio (2021), market creation for green hydrogen requires strategic policy support, such as guaranteed off-take agreements or mandates that compel certain industries to incorporate hydrogen into their energy mix. For instance, implementing renewable hydrogen quotas for chemical and petrochemical industries, where hydrogen is already used as a feedstock but produced from fossil fuels, would create immediate demand without requiring major technological shifts.

2.3 Ammonia

In order to address some of the barriers hindering the widespread adoption of hydrogen, ammonia (NH_3) is increasingly being proposed as a viable hydrogen carrier (Aziz; Wijayanta; Nandiyanto, 2020; Bañares-Alcántara; Salmon; Valera-Medina, 2021).

Ammonia possesses advantageous properties that facilitate its handling. Bartels (2008) mentions the fact that ammonia has 1.5 times higher volumetric energy density than liquefied

hydrogen, making it more efficient to store and transport. Additionally, it can be liquefied under relatively mild conditions compared to hydrogen. Liquid hydrogen needs to be kept at -253°C, while ammonia can be stored as a liquid at -33°C under atmospheric pressure or at room temperature with 10 bars of pressure, which is considerably more cost effective.

Ammonia also has a more favorable safety profile. MacFarlane et al. (2020) cite that although it is classified as a hazardous substance and requires careful handling, ammonia has a higher auto-ignition temperature, a lower flammability range, and a lower gas density than air, making it less likely to ignite or explode. The author also mentions its potent smell as an advantage, since it can be felt from even very low concentrations (5 ppm) still far from the levels where it is considered dangerous to life and health (300 ppm). A report by Duijm, Markert and Paulsen (2005) concluded that the risk associated the use of ammonia as a fuel was comparable and in some cases lower than that of liquified petroleum gas (LGP).

2.3.1 Current state of the industry

Ammonia currently plays a foundational role in the global agricultural sector, serving as a key feedstock for fertilizer production. Its significance in this domain stems from its capacity to synthesize nitrogen-based fertilizers, which are critical for sustaining global food production (see figure 9). Approximately 80% of the global ammonia production, totaling around 175 million metric tons annually, is dedicated to this purpose (Smith; Hill; Torrente-Murciano, 2020). This dependence on ammonia-derived fertilizers was a cornerstone of the Green Revolution and remains vital to modern agricultural practices (MacFarlane et al., 2020).

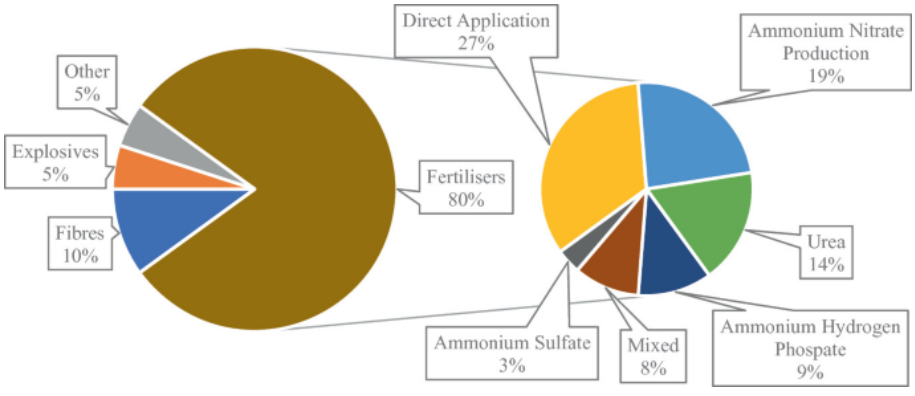

Figure 9: Ammonia uses as of 2020
Source: (Dincer et al., 2022)

Ammonia is the second most produced chemical product globally by total mass, just behind sulphuric acid. It is mainly produced by the the Haber-Bosch process, which synthesizes ammonia by reacting hydrogen with nitrogen under high temperature and pressure. As discussed

in Section 2.2.1, the hydrogen feedstock predominantly originates from fossil fuels, including natural gas, coal, and oil. This reliance on fossil fuels makes ammonia production a significant contributor to greenhouse gas emissions, accounting for approximately 1.2% of global CO_2 emissions (Smith; Hill; Torrente-Murciano, 2020). These emissions arise from both the hydrogen production process and the fossil fuels used as energy sources for the Haber-Bosch process.

Unlike hydrogen, which lacks established supply chains, ammonia is already a widely traded commodity with well-established global markets. According to the IEA (2021), around 20 Mt of ammonia were traded globally in 2019, representing about 10% of total production. The IEA notes that this trade volume reflects significant geographical disparities in production costs, driven by variations in natural gas availability and proximity to demand centers. Countries with abundant natural gas reserves, such as those in the Middle East and North Africa, have a competitive advantage in producing ammonia at relatively low costs, exporting it to regions where local production is less economical. The maturity of ammonia storage, transport, and distribution infrastructure, developed over decades of industrial use, further facilitates its global trade. This established network includes pipelines, refrigerated shipping, and storage terminals, positioning ammonia as a practical and scalable commodity for international markets.

2.3.2 Proposed applications

Besides its traditional role as a fertilizer feedstock, ammonia can act both as a direct fuel and a hydrogen carrier

As a fuel, ammonia offers opportunities for decarbonization due to its combustion characteristics, which release only nitrogen and water, with no direct carbon emissions. However, its low flame speed and high ignition energy pose challenges, necessitating innovations in combustion technology. Current research focuses on ammonia-fueled turbines, internal combustion engines mainly for freight, and ammonia-hydrogen blends, aiming to enhance efficiency while mitigating nitrogen oxide (NOx) emissions, a critical environmental concern (Valera-Medina et al., 2018).

Blending ammonia with hydrogen or methane has been proven effective in improving flame stability and increasing burning velocities, addressing its low reactivity while maintaining carbon neutrality. Catalytic combustion, leveraging metal oxides, has emerged as a promising strategy, reducing NOx emissions and enabling efficient combustion at lower temperatures. These advancements highlight ammonia's adaptability for use in existing and novel systems, including gas turbines and industrial furnaces (Aziz et al., 2023).

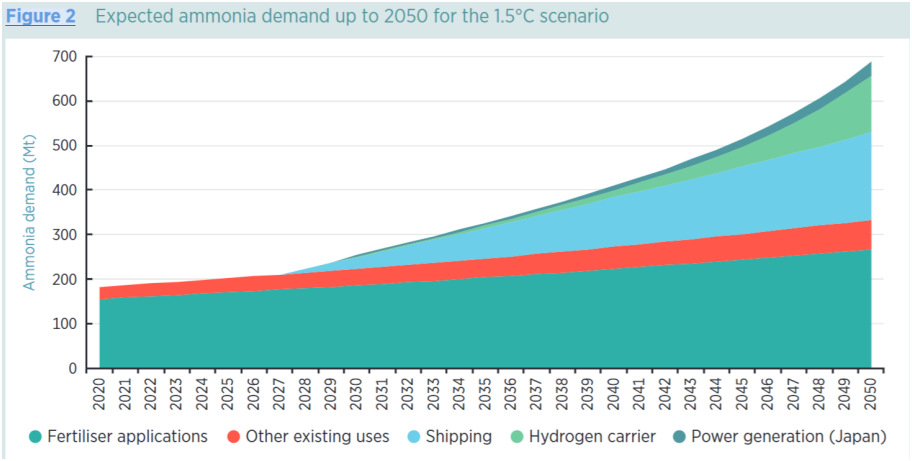

Figure 10: Projection of ammonia demand until 2050
Source: (Rouwenhorst; Castellanos, 2022)

As a hydrogen carrier, ammonia offers a range of technically viable pathways for hydrogen generation, supporting the broader deployment of hydrogen in various applications.

Thermal cracking is the most established and direct method to generate hydrogen from ammonia. This process involves heating ammonia to high temperatures (700–1000°C) to facilitate its decomposition into nitrogen and hydrogen:

$$2NH_3 \rightarrow N_2 + 3H_2$$

A critical component of this process is the use of catalysts to lower the activation energy, improve conversion efficiency, and reduce operational costs. Transition metal-based catalysts, particularly ruthenium on carbon supports or nickel alloys, are widely researched for their superior performance. Despite its technical maturity, thermal cracking's high energy demand remains a challenge. Efforts are being directed toward integrating waste heat recovery systems or coupling the process with renewable electricity to improve sustainability (Aziz et al., 2023).

Electrochemical processes for ammonia decomposition have also gained attention due to their compatibility with renewable energy sources and modular scalability. Solid oxide electrolysis cells (SOECs) and proton-conducting ceramic electrolysis systems operate at intermediate to high temperatures (500–800°C), leveraging electricity to dissociate ammonia into nitrogen and hydrogen. The reaction in such systems can be expressed as:

$$2NH_3 \rightarrow N_2 + 3H_2 + 3e^-$$

This process is particularly efficient in terms of energy use, as it combines the benefits of

direct ammonia decomposition with electrochemical energy conversion. SOECs, for example, utilize solid electrolytes to facilitate ionic conduction while achieving high hydrogen purity. However, challenges such as electrolyte stability, degradation at high temperatures, and the development of low-cost materials are still areas of ongoing research (Aziz et al., 2023)

Despite its potential, ammonia's adoption faces infrastructural and economic challenges. The retrofitting of existing power plants to accommodate ammonia co-firing and the establishment of new infrastructure for storage and transportation are necessary for scaling its deployment. Furthermore, public acceptance and regulatory alignment remain critical, given ammonia's toxicity and the perceived risks associated with its use. Addressing these challenges will require collaborative efforts across industry, academia, and policymakers, ensuring that ammonia's benefits are realized within a framework of safety and sustainability (Aziz et al., 2023).

2.4 Economic evaluation

2.4.1 Levelized cost of energy (LCOE)

The Levelized Cost of Energy (LCOE) is a key metric used to evaluate the competitiveness and feasibility of energy projects. It represents the cost per unit of energy produced over a project's entire lifespan, factoring in capital, operational, and financing expenses. However, it generally focuses on plant-level costs and does not account for additional investments required at the system level, such as upgrades to transmission and distribution grids or other reconfigurations.(Aldersey-Williams; Rubert, 2019)

In general terms, LCOE is calculated by dividing the lifetime costs of the plant by its lifetime energy production as shown in the equation below. (Shen et al., 2020)

$$LCOE = \frac{\text{Lifetime costs}}{\text{Lifetime energy production}}$$

Various private sector actors and international organizations regularly publish data on LCOE, such as Lazard (2024) , IEA (2020) and Timilsina (2020) from the World Bank. The topic has also been extensively discussed in numerous academic studies (Leal, Rego and Ribeiro (2017), Ueckerdt et al. (2013), Shen et al. (2020)). In recent years, the reported numbers for the levelized cost gap between thermal power generation and renewable energy sources has narrowed significantly. In the figure 11, we can find the evolution of the numbers reported yearly by Lazard, showing a steady decrease in the cost of renewable (notably solar PV and onshore wind) driven by advancements in technology, commercial innovation, and changes in revenue

support mechanisms that have facilitated lower-cost project financing. (Lazard, 2024)

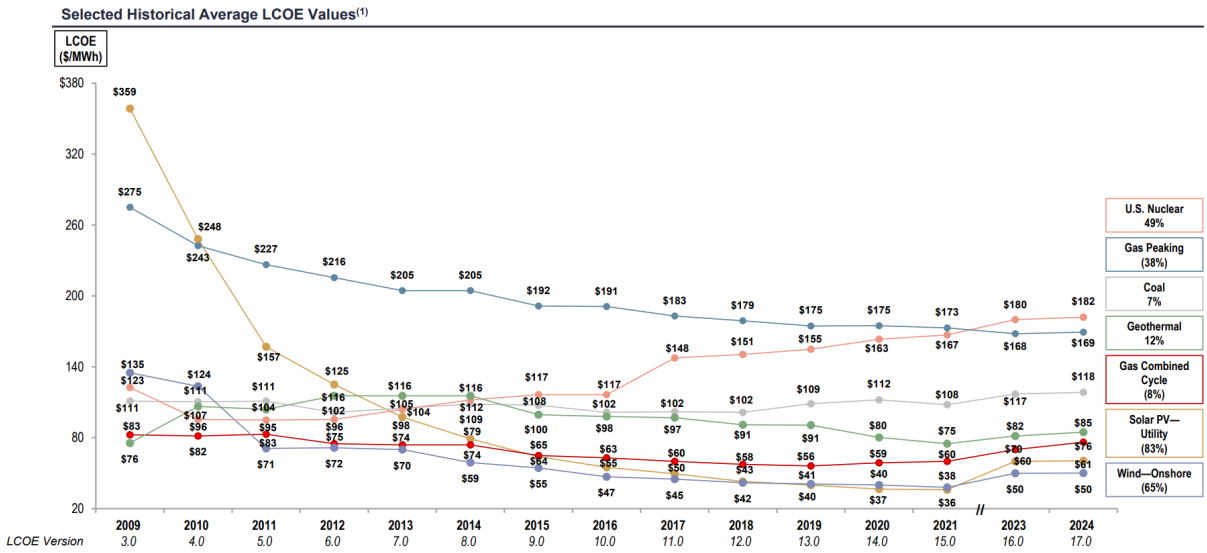

Figure 11: Evolution of LCOE values during the last 15 years.
Source: (Lazard, 2024)

In practice, the literature (Aldersey-Williams and Rubert (2019), Shen et al. (2020)) identifies two main approaches to break down the calculation of LCOE. The "discounting" method, suggested by the United Kingdom Department for Energy Security and Net Zero (DESNZ) and the "annuitization" method, suggested by the United States Department of Energy's National Renewable Energy Laboratory (NREL).

DESNZ Method (UK)

This definition was first developed by the UK Department of Energy and Climate Change (DECC), which later became the current Department for Energy Security and Net Zero (DESNZ). DECC (2013) employs a methodology that defines LCOE as "the discounted lifetime cost of ownership and use of a generation asset, converted into an equivalent unit of cost of generation". This approach discounts both costs and energy production over the lifetime of a project to produce a real cost per unit of energy. The formula for the calculation of the metric can be found below.

$$LCOE_{\text{DESNZ}} = \frac{NPV_{\text{costs}}}{NPE} = \frac{\sum_{t=1}^{T} \frac{C_t + O_t + V_t}{(1+r)^t}}{\sum_{t=1}^{T} \frac{E_t}{(1+r)^t}}$$

Where:

- C_t represents the capital costs in year t,
- O_t represents the operating and maintenance costs in year t,

- V_t represents the variables costs (fuels, taxes, carbon) in year t,
- E_t is the energy output in year t,
- r is the discount rate,
- T is the lifetime of the project.

Aldersey-Williams and Rubert (2019) develops a theoretical justification for this approach by deriving it in the following manner. In essence, when the project's internal return rate (IRR) is equal to the discount rate, it follows that $NPV_{\text{revenues}} = NPV_{\text{costs}}$. This leads to the LCOE expression in terms of revenues:

$$LCOE = \frac{NPV_{\text{revenues}}}{NPE}$$

This value can be interpreted as the constant energy price in real terms required for the project's revenues to match the IRR equating to the discount rate. Therefore, through this approach, the LCOE essentially represents the minimum required real price for a project to achieve the desired return.

NREL Method (US)

In contrast, the National Renewable Energy Laboratory (NREL) in the United States uses an alternative approach that focuses on the annualized cost of energy. NREL (2018) describes a method that calculates capital costs using a capital recovery factor, while operating and fuel costs are handled separately to compute the LCOE on an annual basis. Their formulation for the LCOE is:

$$LCOE_{NREL} = \underbrace{\frac{C_o \cdot CRF + O}{CF \cdot 8760}}_{\text{Fixed component}} + \underbrace{f \cdot h + V}_{\text{Variable component}}$$

Where:

- C_o is the overnight capital cost,
- CRF is the capital recovery factor
- O is the fixed operating cost,
- CF is the capacity factor,
- f is the fuel cost,

- h is the heat rate,
- V is the variable operating cost,
- 8760 is the number of hours in a year.

The capital recovery factor, which converts the overnight capital cost into an equivalent annual payment over the project's lifetime, is calculated as follows:

$$CRF = \frac{i(1+i)^n}{(1+i)^n - 1}$$

Where:

- i is the interest rate,
- n is the number of payments made to repay the capital.

According to the NREL (2018), this formulation represents "the minimum price at which energy must be sold for an energy project to break even." In other words, it signifies the energy price necessary for a project to exactly cover its annual operating costs and the portion of capital costs, including financing expenses, allocated to that year.

While both the NREL and DESNZ methods aim to determine the cost per unit of electricity, they differ in their treatment of costs, discounting mechanisms, and representation of energy production. The DESNZ method's comprehensive lifetime analysis provides a nuanced understanding of the project's financial performance over time, accommodating variations in annual costs and outputs. This makes it particularly suitable for technologies with non-uniform performance or costs, such as renewable energy sources with intermittent outputs or equipment degradation over time.

Conversely, the NREL method offers simplification and practicality. By focusing on annual costs and outputs, it is effective for assessing technologies with stable performance and costs, providing a clear and concise cost metric for quick comparisons. However, it assumes that the capacity factor and costs remain constant over time, which may not hold true for all technologies or market conditions.

As highlighted by Shen et al. (2020), if certain conditions are met, the two methods can yield similar LCOE estimates. These conditions include:

1. The annual energy output and cost of the project are constant;

2. All capital expenditures occur in the first year;

3. Capital recovery starts immediately with a financing term equal to the project's operating life

4. There are no decommissioning costs

2.4.1.1 Limitations of the classical LCOE

Despite its widespread use among policymakers and industry stakeholders, the Levelized Cost of Energy (LCOE) as an economic evaluation metric has been critiqued by scholars for several inherent limitations.

One notable shortcoming of the LCOE is its inadequacy in comparing intermittent energy sources with dispatchable ones. As highlighted by Joskow (2011), the LCOE overlooks the varying economic value of electricity generated at different times. The wholesale electricity market is characterized by significant price fluctuations throughout the day and year, driven by changes in demand. Dispatchable technologies (coal, gas, nuclear) have the ability to produce power when demand, and consequently the price of electricity is highest, thereby maximizing revenue. In contrast, intermittent technologies like wind and solar produce electricity based on environmental conditions (e.g., wind speed, sunlight), which often do not align with periods of peak demand. The author argues that, with the availability of competitive electricity markets and advanced models for forecasting prices and demand, there is no need to rely on the metric of levelized costs. Instead, the economic evaluation of any power generating technology should consider both, costs and value of that technology. The work of Reichelstein and Sahoo (2015) goes on this same line by proposing a co-variation coefficient to correct the LCOE of intermittent sources. This coefficient adjusts for the temporal synergies between electricity generation and price fluctuations, demonstrating that intermittent sources may be undervalued when their generation aligns with high-price periods (e.g., solar during afternoon peak hours). Their analysis suggests that traditional LCOE metrics undervalue solar PV's competitiveness by 10-15% and overestimate the value of wind energy, which often generates power during low-demand periods.

Another important aspect not taken into account by the standard formulations of the LCOE relates to the system integration costs. Those costs encompass the additional expenses required to maintain grid stability and ensure adequate power supply in the presence of fluctuating renewable generation. These include the costs of balancing services, construction of new transmission lines, grid reinforcement, and adequacy costs for backup capacity. Ueckerdt et al.

(2013) propose a top-down approach to determine integration costs, contrasting with the typical bottom-up methodology used in engineering studies. Instead of calculating each cost component separately, this approach suggests comparing two system states, one with and one without the renewable source, and assessing the additional system costs introduced by it.

The LCOE has also been critiqued for its lack of consideration of more indirect factors, often treated as external to energy systems, such as environmental impacts and social costs. To address this, Roth and Ambs (2004) propose a full-cost pricing approach that integrates the Life Cycle Costing (LCC) method to account for externalities within the LCOE framework. This approach incorporates external costs related to emissions, land use impacts, water-related environmental effects, and energy security, thus providing a comprehensive view of total costs. By assigning these costs to pollutants such as CO_2, SO_2, NOx, and particulate matter, the model converts environmental impacts into monetary values that can be directly included in the LCOE. In addition, non-environmental externalities, including government spending on fuel security and the economic risks of foreign energy dependency, are integrated to capture the broader socio-economic impacts of reliance on fossil fuels.

A final limitation in the conventional LCOE formulation is its deterministic nature, relying on single-point estimates, or best-guess values, for all input variables, such as capital cost, fuel price, capacity factor, and the discount rate (Barros et al., 2016). Although this approach allows for a simplified estimation, these input parameters are inherently uncertain and can fluctuate significantly over time, particularly for long-term investments such as power plants (Heck; Smith; Hittinger, 2016). Several studies have sought to address this gap and their approach will be further developed in the following section.

2.4.1.2 Stochastic LCOE

To address these limitations, one of the proposed ways to overcome the shortcomings of traditional LCOE calculation is to model the input parameters as random variables that follow an appropriate probability distribution (Heck, Smith and Hittinger (2016), Ozato et al. (2023)). This subsection explores the integration of stochastic modeling into LCOE calculations, highlighting its advantages, methodologies, and implications for the energy sector.

Integrating stochastic modeling into LCOE provides several strategic advantages for investors and policymakers. For example, the study by Heck, Smith and Hittinger (2016) underscores how stochastic LCOE allows for risk-adjusted cost estimates, which are essential for project financing and investment decisions in volatile markets. By enabling the calculation of confidence intervals for the results, this approach offers insights into the range of poten-

tial LCOE outcomes under varying assumptions and risk levels. Moreover, Lucheroni and Mari (2017) demonstrate how stochastic LCOE models can enhance portfolio management by identifying diversification opportunities within an energy portfolio, thus mitigating financial exposure to individual market risks such as fuel price volatility and regulatory changes. By quantifying the effects of CO_2 volatility, they demonstrated how nuclear power could act as a hedge against fossil fuel price risks.

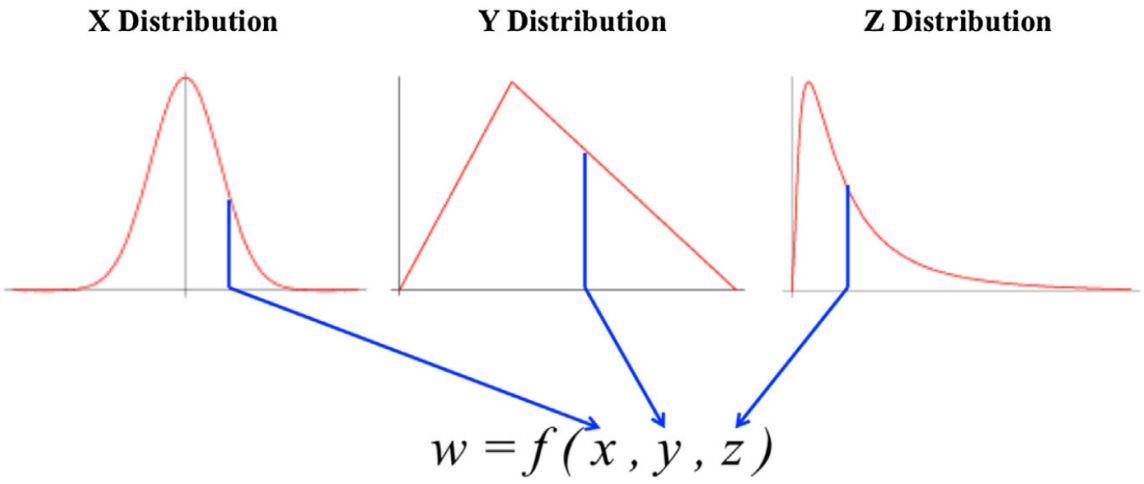

Figure 12: Modeling of the stochastic LCOE as the function f
Source: (Heck; Smith; Hittinger, 2016)

In applying stochastic LCOE, several core variables are transformed into probabilistic inputs, as illustrated by the figure 12. Capital expenditure (CAPEX), for example, is modeled stochastically due to substantial uncertainties tied to factors such as technology, labor, and material costs, all of which are susceptible to economic conditions and technological advancements. Heck, Smith and Hittinger (2016) illustrate this variability with the example of some nuclear power plants in the United States, where construction ultimately resulted in cost overruns exceeding 100% by project completion. Such significant variability underscores the necessity of incorporating probabilistic modeling to provide a realistic risk assessment. Another essential variable in stochastic LCOE is the capacity factor, which denotes the ratio of actual energy output to maximum potential output. This factor is particularly volatile in renewable projects, where weather conditions at the considered location can drastically impact generation (Heck; Smith; Hittinger, 2016) . Lee and Ahn (2020) demonstrate how capacity factor variability in solar PV projects can drive substantial changes in LCOE, underscoring the need for probabilistic modeling to accurately reflect seasonal and geographical variations in solar irradiance. In the case of fossil-fuel-based generation, fuel and carbon prices are critical uncertainties, as they are highly sensitive to regulatory changes and market conditions. Lucheroni and Mari (2017) show how carbon price volatility can affect the financial outcomes of this kind of project and

incentivize the diversification into CO_2 free sources.

According to Lee and Ahn (2020), selecting an appropriate probability distribution for the input variables can be informed by available data, expert judgment, or a combination of both. Key considerations for this judgment include whether the data are discrete or continuous, bounded or unbounded, unimodal or multimodal, and whether the distribution is symmetrical or skewed.

The triangular distribution is frequently used in the literature (Heck, Smith and Hittinger (2016), Barros et al. (2016), Ozato et al. (2023)) particularly when detailed historical data is limited. Its popularity stems from its simplicity, as it requires only the estimation of minimum, most likely, and maximum values, making it straightforward to define with limited information. Additionally, the triangular distribution can accommodate asymmetry, which is crucial for representing situations where the distances between the two extremes and the distribution mode differ.

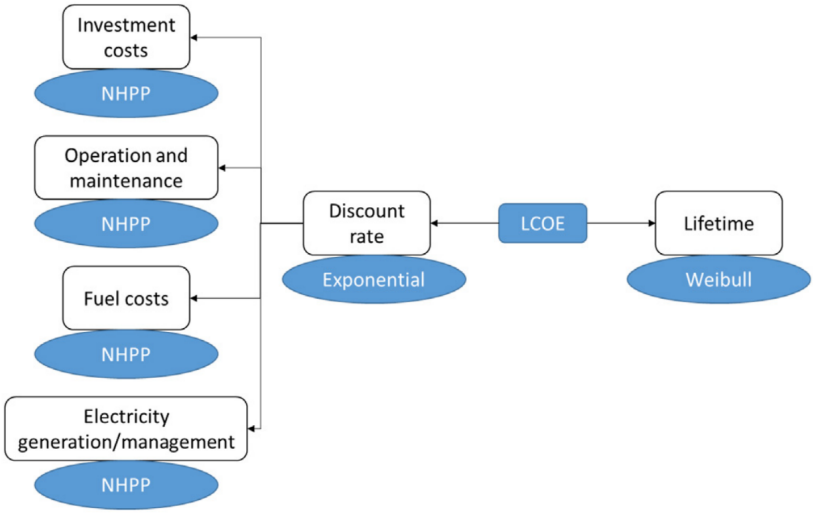

Figure 13: Modeling framework for the stochastic LCOE
Source: (Tazi; Safaei; Hnaien, 2022)

In their work, Tazi, Safaei and Hnaien (2022) propose an innovative methodology for modeling the components of LCOE, including CAPEX (capital expenditures), OPEX (operating expenditures), fuel costs, and energy generation. This approach employs a non-homogeneous Poisson process (NHPP) to describe the stochastic behavior of these components, as illustrated in Figure 13.

An NHPP is a type of stochastic process where the arrival rate of events, denoted by $\lambda(t)$, is time-dependent, as opposed to the homogeneous Poisson process where λ remains constant over time. This flexibility makes it ideal for representing dynamic systems across diverse en-

gineering and reliability contexts. For example, in repairable systems, NHPPs enable the modeling of failure times with greater precision than homogeneous Poisson processes, as they can accommodate complex failure behaviors influenced by system wear and aging of equipments (Lawless; Crowder, 1995). Similarly, in materials science, NHPPs have also proven effective in studying creep rupture under sub-critical external loads, where the failure rate accelerates as materials approach their breaking point (Kun; Costa; Andrade, 2013).

In mathematical terms, the modeling proposed by Tazi, Safaei and Hnaien (2022) for each component (investments in this example) follows this structure:

$$E\left(\int_0^\infty I(t)e^{-rt}\,dN_1(t)\right) = \int_0^\infty I(t)G(t)e^{-rt}\lambda_1(t)\,dt$$

- $N_1(t)$: The NHPP representing the number of investment events up to time t.
- $\lambda_1(t)$: The time-dependent rate function for investments.
- $I(t)$: The investment expenditure at time t.
- r: The continuous discount rate.
- $G(t)$: A function representing the probability that the system is operational at time t .

In this equation, the left-hand side represents the expected discounted investment costs over time, accounting for the random occurrence of investment events modeled by $dN1(t)$. The right-hand side simplifies this expectation by integrating over time with the rate function $\lambda_1(t)$ and the operational probability $G(t)$.

Another choice made by Tazi, Safaei and Hnaien (2022) is the modeling of the project's lifetime as a random variable following a Weibull distribution. The authors highlight the Weibull distribution's popularity as a lifetime model and its flexibility in representing different failure rate behaviors (increasing, decreasing, or constant) depending on a shape parameter.

Putting it all together, their formulation of the stochastic LCOE is given by:

$$\text{LCOE} = \frac{\int_0^\infty \left(I(t)\lambda_1(t) + M(t)\lambda_2(t) + F(t)\lambda_3(t)\right)G(t)e^{-rt}\,dt}{\int_0^\infty E(t)\lambda_4(t)G(t)e^{-rt}\,dt}$$

Where:

- $I(t)$: Investment costs at time t.
- $M(t)$: Maintenance costs at time t.

- $F(t)$: Fuel costs at time t.
- $E(t)$: Energy generation at time t.
- r: The continuous discount rate.
- $G(t)$: the probability that the system is operational at time t
- $\lambda_i(t)$: Time-dependent rate functions for the different cost components.

In order to estimate the outcomes of the stochastic LCOE modeling, Monte Carlo simulation is the predominant technique, as highlighted in various studies (Heck, Smith and Hittinger (2016), Lucheroni and Mari (2017), Ioannou, Angus and Brennan (2017), Ozato et al. (2023), Lee and Ahn (2020)).

The Monte Carlo method relies on the law of large numbers, which states that the sample mean of independent, identically distributed random variables converges to the expected value as the sample size grows indefinitely (Dekking et al., 2006). For a random variable X with probability density function $f_X(x)$ and an arbitrary function $g(X)$, the expected value $E[g(X)]$ is given by:

$$E[g(X)] = \int_{x \in X} g(x) f_X(x)\, dx$$

As described in Lee and Ahn (2020), through Monte Carlo simulation, it is possible to estimate the value of this integral without having to directly calculate the antiderivative of the function $g(x)f_X(x)$. The Monte Carlo method approximates $E[g(X)]$ by taking n independent samples from X, denoted $(x_1, x_2, \ldots, x_n)$, and computing the average of $g(x)$ values over these samples. This approximation, called the Monte Carlo estimator, is defined as:

$$\tilde{g}_n(X) = \frac{1}{n} \sum_{i=1}^{n} g(x_i)$$

As $n \to \infty$, the Monte Carlo estimator $\tilde{g}_n(X)$ converges to $E[g(X)]$ due to the law of large numbers and an estimate of the LCOE is obtained.

3 METHODOLOGY

In this chapter, we define the modeling framework, present the collected data and assumptions underpinning the models, and discuss the operation of the implemented simulation algorithm. Two hydrogen production pathways are analyzed: Proton Exchange Membrane (PEM) water electrolysis, which serves as the benchmark, and Alkaline (ALK) ammonia electrolysis, the technology under evaluation in this study.

3.1 LCOH modeling framework

The framework adopted to calculate the levelized cost of hydrogen was the one implemented by Kee and Penev (2023), from the National Renewable Energy Laboratory of the United States (NREL). It consists of the Python library *ProFAST*, which is available under a free license and can be installed in a local computer. The library builds upon the established Excel-based calculator *H2FAST*, also developed by the NREL, and has been applied in previous studies for the economic evaluation of hydrogen projects (Pratt; Luzi; Freeburg, 2017; Hunter et al., 2020).

ProFAST calculates the levelized cost of production or financial performance based on input prices, incorporating key inputs like capital expenditures, operating costs, and financing structures. Its availability in the form of a Python library allows the LCOH calculation to be easily combined with stochastic modeling of the inputs.

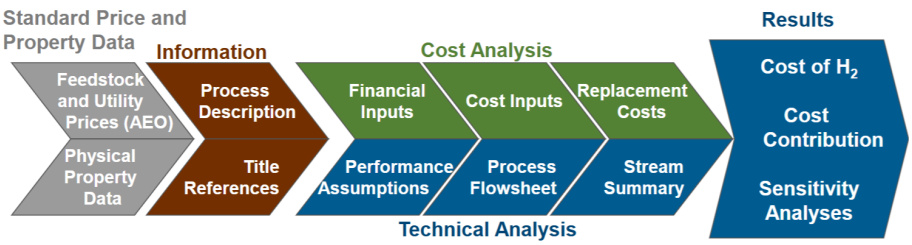

Figure 14: Steps for the modeling in H2FAST
Source: (Penev, 2020)

The library can be employed in two main modes of functioning: price setter or price taker. In the price setter mode, the user pre-defines the commodity price, and the tool calculates the resulting internal rate of return (IRR) for the project. Conversely, in the price taker mode, the model determines the commodity's break-even price to achieve a specified discount rate. For this study, the price taker mode will be used, as the LCOH represents a break-even price that reflects the project's economic viability.

3.1.1 Required parameters and their integration in *ProFAST*

To perform its calculations, *ProFAST* requires a comprehensive set of input parameters that can be grouped into distinct categories. The library integrates these inputs programmatically, enabling precise customization for specific projects.

At a minimum, the following parameters are required for *ProFAST* to function:

- **System Configuration**:
  - **Capacity**: Daily production capacity (e.g., in kg/day for hydrogen).
  - **Long-Term Utilization**: Operational capacity factor, representing the proportion of time the plant operates at full capacity.
  - **Operating Life**: Total duration of project operation, in years.
  - **Installation Months**: Time required for installation and commissioning, in months.
- **Economic Parameters**:
  - **General Inflation Rate**: A base value for cost escalation applied to various project expenses.
  - **Capital Expenditures (CAPEX)**: Total initial investment cost, defined along with depreciation method (e.g., linear) and period.
  - **Operating Expenditures (OPEX)**: Recurring costs such as maintenance, labor, and utilities, with escalation rates if applicable.
  - **Financing Structure**: Debt-to-equity ratio, interest rates, and tax rates.
- **Feedstock Requirements**:
  - **Feedstock Name and Usage**: Key raw material inputs (e.g., electricity, water) with specified consumption rates.
  - **Feedstock Costs**: Unit prices for feedstocks, with optional escalation rates.

- **Financial Objectives**:
  - **Discount Rate**: Target rate used to evaluate financial performance.
  - **Commodity Price**: Initial price or break-even price calculation, depending on the mode of operation.

Beyond the minimal inputs, *ProFAST* allows users to refine the analysis through additional parameters:

- **Incentives**: Includes one-time capital grants, annual subsidies, or tax credits.
- **Incidental Revenues**: Supplemental income sources, such as byproduct sales.
- **Tax Considerations**: Options to monetize tax losses, specify capital gains tax rates, or adjust tax carryforward rules.
- **Fixed and Variable Costs**: Detailed accounting for annualized replacements and other fixed operational expenses.

3.1.2 How *ProFAST* Uses These Inputs

ProFAST projects cash flows by synthesizing detailed input parameters into a comprehensive financial model that spans the entire operational life of the hydrogen production system. The model begins by calculating annual revenues, using the initial hydrogen price and projected production volumes, adjusted for factors such as demand ramp-up periods, long-term utilization rates, and potential incidental revenues from by-products such as oxygen. Operating expenses are then subtracted from revenues to derive the gross operating margin. These expenses are determined based on feedstock consumption rates (e.g., electricity and water), labor costs, maintenance, rent, and other variable and fixed costs, each escalated according to inflation rates or input-specific escalation factors. Capital expenditures, including installation costs and refurbishments, are integrated into the model through depreciation schedules, allowing *ProFAST* to estimate tax shields that lower taxable income.

The model can also accounts for financing details, such as debt/equity ratios, interest rates, and cash-on-hand requirements, which influence the cost of capital and subsequent cash flow calculations. By combining these elements, *ProFAST* constructs a year-by-year projection of cash inflows and outflows, factoring in inflation and applying discount rates to reflect the time value of money. This results in a detailed net cash flow profile that forms the foundation for profitability assessments.

In the price taker mode, *ProFAST* calculates the break-even price by iteratively adjusting the hydrogen price until the net present value (NPV) of the project equals zero. It uses the NPV formula, summing discounted cash flows over the project's lifetime, where cash flows are determined by subtracting operating and capital costs from revenues based on the current price. The process involves the bisection method for numerical root-finding, refining the price based on whether the NPV is positive or negative until it converges to a near-zero tolerance (e.g., \$0.01).

3.2 Data collection and assumptions

This section outlines the values and assumptions used as inputs for the model in *ProFAST*. Initially, we define the parameters shared between the two systems under comparison (water and ammonia electrolysis), followed by a detailed specification of the parameters unique to each individual system.

3.2.1 Shared modeling assumptions

3.2.1.1 Scenario definition

Electricity is a critical factor in the production of green hydrogen, significantly shaping both the economic feasibility and environmental impact of the process. To capture the range of possible outcomes, this study considers two scenarios for electricity generation. Each scenario reflects a distinct approach to sourcing electricity, with implications for costs and operational performance.

The first scenario considers electricity sourced directly from the **national grid**. In Brazil, over 90% of the total electricity produced originates from renewable sources (Ministry of Mines and Energy, 2023), meeting the green hydrogen qualification criteria established by the EUROPEAN COMISSION (2023). In this scenario, the capacity factor for the grid source is stable and assumed to be 97%, as adopted by Hubert et al. (2024). Regarding electricity costs, the Brazilian tariff system separates pricing into two components: the *TUSD*, which covers energy transmission costs, and the *TE*, which reflects the cost of energy generation. The *TUSD*, regulated by the Brazilian Electricity Regulatory Agency (ANEEL), currently stands at 570 BRL/MWh (98.5 USD/MWh) for the state of Bahia (ANEEL, 2024). Conversely, the *TE* exhibits variability. Using data from Dcide (2024) on the long-term forward price curve for conventional electricity, the *TE* component will be sampled from the distribution shown in Figure 15.

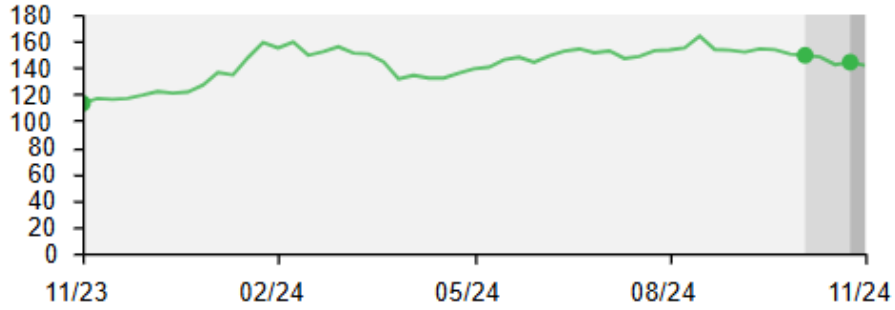

Figure 15: Long term price forward curve for grid electricity (BRL/MWh)
Source: (Dcide, 2024)

The second scenario considers electricity sourced through a power purchase agreement (PPA) with a **wind power** supplier. In order to set te *TE*, or generation tariff, we use as reference a recent PPA agreement for a mining project in Brazil, which established a fixed price of 29 USD/MWh (Reuters, 2022). The *TUSD* for this scenario assumes a subsidized rate, set at 50% of the standard cost, resulting in a total of 400 BRL/MWh (69 USD/MWh) (ANEEL, 2024). Unlike the grid-sourced scenario, where electricity costs vary, the PPA offers fixed costs for energy generation. However, the capacity factor for this scenario is variable, reflecting seasonal and operational variations in wind power availability. The electrolyzer's operational capacity factor is assumed to align with the wind power source. With this approach, we aim to assess if a cheaper electricity source could compensate for a lower utilization of the equipment. We collected data from ONS (2024) on historic values for the monthly capacity factor over the last 4 years for wind plants in the northeast of Brazil and the empirical distribution will be used to sample values for the simulation.

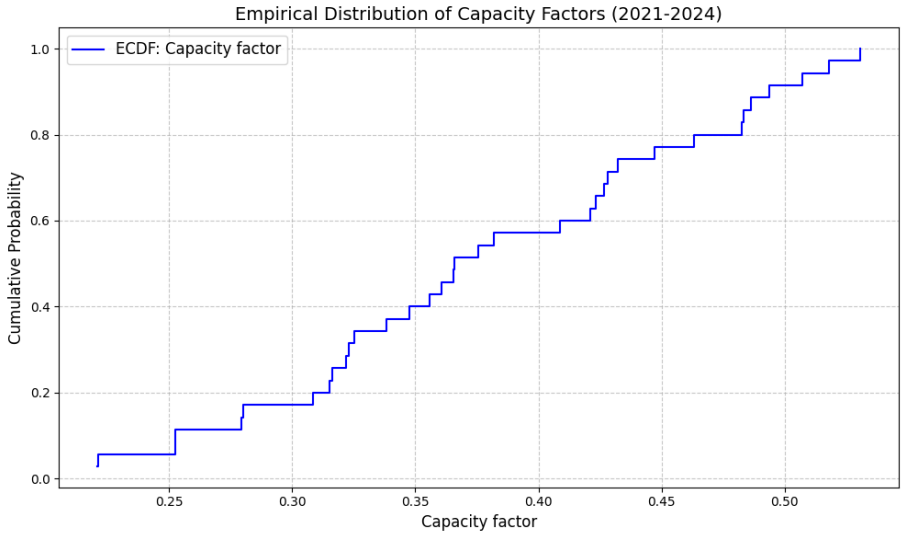

Figure 16: Empirical distribution of monthly capacity factor of wind energy in Brazil (2021-2024)

Source: (ONS, 2024)

	Scenario 1 **Grid electricity**		**Scenario 2** **Wind electricity**	
	Input value	Distribution	Input value	Distribution
Capacity factor	97%	Constant value	Sampled	Empirical from (ONS, 2024)
Electricity cost	TE: sampled	Empirical from (Dcide, 2024)	TE: 29 USD/MWh	Constant value
(TE+TUSD)	TUSD: 98 USD/MWh	Constant value	TUSD: 69 USD/MWh	Constant value

Table 2: Scenarios for electricity source

Source: Elaborated by the author

3.2.1.2 Plant refurbishments

For both hydrogen producing plants, we seek to simulate the impact of refurbishment events during the operational lifetime of both plants.

To achieve this, we employ the stochastic LCOE framework proposed by Tazi, Safaei and Hnaien (2022), which models the disbursement of CAPEX using a non-homogeneous Poisson process (NHPP) characterized by a time-dependent rate function $\lambda(t)$, as detailed in Section 2.4.1.2.

In this approach, the rate function $\lambda(t)$ is interpreted as a failure rate for the system and modeled using the Weibull hazard function. This choice reflects the typical failure dynamics of components over time, with the hazard function expressed as:

$$\lambda(t) = \frac{\beta}{\eta}\left(\frac{t}{\eta}\right)^{\beta-1},$$

where:

- β is the shape parameter that determines the failure rate trend (e.g., increasing, constant, or decreasing over time),
- η is the scale parameter, that defines the characteristic time scale of failures.

To define the appropriate shape of the failure rate, we sought studies reporting statistical data on electrolyzer failures. However, due to the experimental nature of most current plants and their limited time in commercial operation, such data was not readily available. As an alternative, we referenced the findings of Gaonkar et al. (2021), which analyze the failure rates of various electronic components. The study concludes that failure rates for electronics generally follow an increasing trend, driven by factors such as component fatigue, corrosion, and thermal stresses, starting from the moment the system becomes operational. Therefore, we employed the values of $\beta = 3$, signaling an increasing failure trend, and $\eta = 20$, in order to accommodate the typical lifetime of the plants.

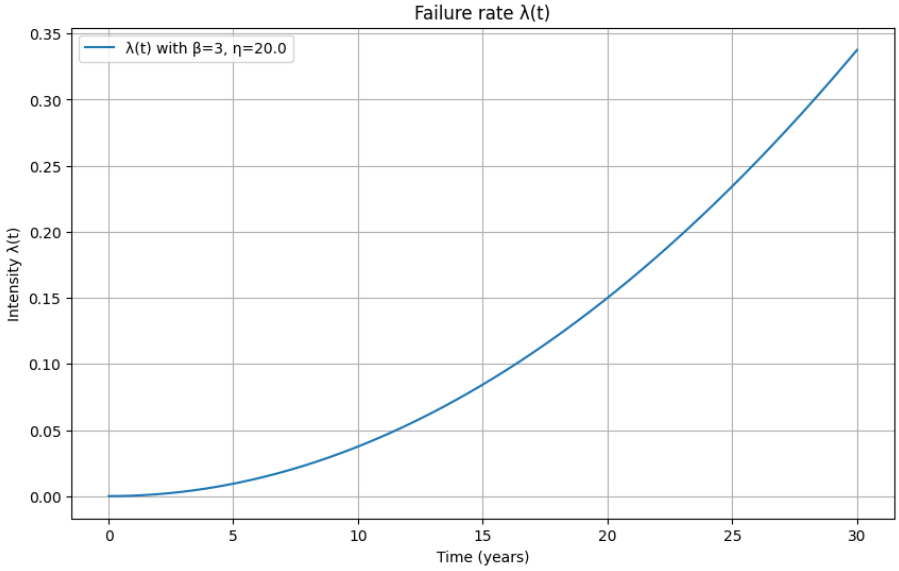

Figure 17: Implemented failure rate

Source: Elaborated by the author

After each refurbishment event triggered by a failure, the corresponding disbursement will be a proportion of the total installed CAPEX and drawn from a uniform distribution to reflect the

variability and uncertainty in costs. After discussion with experts from the Escola Politécnica the proportion was defined to be between 15 to 40% of total CAPEX.

3.2.1.3 Other assumptions

Additional shared assumptions between both plants are related to the macro-economic variables and parameters linked to the financial structure of the projects. The values which were ultimately considered are reconstituted in table 3.

Parameter	Description	Value	Source
General inflation rate	General inflation rate of the dollar	2.1%	(Cleveland, 2024b)
Debt / Equity Ratio	Debt-to-equity ratio for initial financing	1.41	(Damodaran, 2024b)
Debt interest rate	Interest rate for debt	5%	(Hubert et al., 2024)
Income tax rate	Combined tax rate applied to income in Brazil	34%	(Damodaran, 2024a)
Discount rate	Discount rate for financial analysis, taken as the SELIC	11.25%	(CENTRAL BANK OF BRAZIL, 2024)
Operating life	Total project operating life in years	30 years	Assumption
Installation time	Installation time before production (months)	12 months	Assumption

Table 3: Common modeling parameters
Source: Elaborated by the author

3.2.2 Hydrogen from water electrolysis

In modeling hydrogen production through water electrolysis, we adopted a parameter set that reflects the current technological status of proton exchange membrane (PEM) electrolyzers. The system design assumes a centralized hydrogen production plant with a nominal capacity of 50,000 kg/day, corresponding to an installed system power requirement of approximately 115 MW. This capacity reflects a large-scale operation aligned with the scale-up trends in the U.S. and Brazilian markets

Electrolyzer efficiency is a critical parameter, and the specific energy consumption for hydrogen production was set at 57.5 kWh per kilogram of hydrogen, as derived from empirical data from (Hubert et al., 2024). This value includes both stack efficiency (electricity consumption within the electrolyzer stack) and balance-of-plant (BOP) energy consumption. The efficiency metric was selected to align with recent industrial deployments and conservative estimates to capture real-world performance variability.

Regarding water usage, the electrolysis process requires approximately 9 liters of water per kilogram of hydrogen produced. The cost of water was set at $0.002 per liter, based on stoichiometric requirements and standard industrial water pricing. These inputs contribute to the

ancillary costs of operation, which, while small in comparison to electricity costs, are essential for a comprehensive economic modeling.

Capital expenditure (CAPEX) was modeled using an installed system cost of $2,000 per kilowatt of capacity, reflecting the PEM electrolyzer stack, BOP components, and installation costs. Annual maintenance costs were assumed to be 5% of the total CAPEX, consistent with industry benchmarks and previous techno-economic analyses. The operational lifetime of the electrolyzer was set at 30 years, with stack replacements simulated by the non-homogeneous Poisson process.

Parameter	Description	Value	Source
Plant maximum capacity	Daily production capacity	50,000 kg of H_2	(Hubert et al., 2024)
System cost	Cost per kW for entire system (PEM stack, BOP etc)	2,000 USD/kW	(Hubert et al., 2024)
Maintenance cost	Annual maintenance cost	5% of CAPEX	(Hubert et al., 2024)
Water usage	Water consumption per kg of H_2 produced	9l/kg of H_2	(Hubert et al., 2024)
Water cost	Cost per liter of water	0.002 USD/l	stoichiometry
Electricity usage	Electricity consumption per kg of H_2 produced	57.5 kWh/kg of H_2	(Hubert et al., 2024)

Table 4: Water electrolysis model parameters
Source: Elaborated by the author

3.2.3 Hydrogen from ammonia electrolysis

The core of the ammonia electrolysis system is an alkaline electrolyzer stack, as this is the most mature technology currently available for the process (Kanaan et al., 2023). The system design assumes a centralized hydrogen production plant with a nominal capacity of 50,000 kg/day, consistent with the scale of operation modeled for water electrolysis. This capacity ensures a comparable analysis between the two production pathways.

The performance of ammonia electrolysis relies heavily on energy efficiency of the process and the effective use of feedstock. Ammonia electrolysis requires 13.35 kWh of electricity per kilogram of hydrogen produced, which includes the energy demands for ammonia breakdown, hydrogen extraction, and supporting operations. For each kilogram of hydrogen, 5.75 kg of ammonia is consumed, consistent with stoichiometric calculations.

As the cost of the ammonia feedstock is still quite uncertain and it is expected to weigh heavy in the final result of the LCOH, it will be modelled stochastically in our simulation. Rouwenhorst and Castellanos (2022) provided a range from $720-1400 per ton of NH_3. Meanwhile, Kanaan et al. (2023) used the value of $1000 per ton in their base case. Therefore, the cost of green ammonia will be drawn from a triangular distribution in our simulation, with a minimum of $720, a mode of $1,000, and a maximum of $1,400 per ton of green ammonia.

The system's capital expenditure (CAPEX) includes costs for the alkaline electrolyzer stack, balance-of-plant (BOP) components, and associated infrastructure. The alkaline stack is modeled with a cost of $1,000 per kilowatt, while the BOP is assumed to cost five times the stack, reflecting the complexity of auxiliary components such as the electrolyte circulation system and gas purification units. Maintenance costs are modeled at 5% of CAPEX annually, consistent with industry standards for similar technologies.

The parameters are summarized in table 5.

Parameter	Description	Value	Source
Alkalyne stack cost	Cost per kW for Alkalyne Stack	1,000 USD/kW	(Kanaan et al., 2023)
Ammonia usage	Consumption of ammonia per kg of Hydrogen	5.75 kg of NH_3/kg of H_2	(Kanaan et al., 2023)
Green ammonia cost	Cost per ton of ammonia	Triangular(740,1000,1400) USD/t of NH_3	(Kanaan et al., 2023) and (Rouwenhorst; Castellanos, 2022)
Plant maximum capacity	Daily production capacity	50,000 kg of H_2	(Hubert et al., 2024)
System cost	Cost for rest of system (Infrastructure, BOP etc)	5 times electrolyzer	(Kanaan et al., 2023)
Maintenance cost	Annual maintenance cost	5% of CAPEX	(Hubert et al., 2024)
Electricity usage	Electricity consumption per kg of H_2	13.35 kWh/kg of H_2	(Kanaan et al., 2023)

Table 5: Ammonia electrolysis model parameters
Source: Elaborated by the author

3.3 Simulation design

This study employs a Monte Carlo simulation framework to evaluate the levelized cost of hydrogen (LCOH) for two hydrogen production pathways: water electrolysis and ammonia electrolysis. It is is designed to iteratively calculate the LCOH by integrating stochastic variations in critical input parameters, including electricity costs, capacity factors, and refurbishment schedules. The *ProFAST* model serves as the core computational tool, allowing for a dynamic representation of hydrogen production processes, cost structures, and financial metrics. Key inputs are systematically varied across 1,000 simulation iterations for each scenario, generating a statistically robust distribution of LCOH outcomes.

3.3.1 Refurbishment event simulation

To simulate refurbishment events over the operating life T of the equipment, we utilize the thinning algorithm developed by Lewis and Shedler (1979), a method adept at generating event times for an NHPP when the intensity function is complex or lacks an easily invertible cumulative intensity function. The simulation algorithm proceeds as follows:

1. Determine the maximum intensity $\lambda_{\max}$:

Compute the maximum value of the intensity function over the interval $[0,T]$:

$$\lambda_{\max} = \max_{t\in[0,T]} \lambda(t).$$

2. Generate candidate event times:

   Sample N from a Poisson distribution with parameter $\lambda_{\max}T$:

   $$N \sim \text{Poisson}(\lambda_{\max}T).$$

   Generate N candidate event times uniformly distributed over $[0,T]$:

   $$t^{(i)}_{\text{candidate}} \sim \text{Uniform}(0,T), \quad i = 1,2,\ldots,N.$$

3. Thinning process:

   For each candidate time $t^{(i)}_{\text{candidate}}$:

   Compute the acceptance probability:

   $$p^{(i)}_{\text{accept}} = \frac{\lambda(t^{(i)}_{\text{candidate}})}{\lambda_{\max}}.$$

   Draw an uniform random number $u^{(i)} \sim \text{Uniform}(0,1)$.

   Accept $t^{(i)}_{\text{candidate}}$ as an actual event time if:

   $$u^{(i)} \leq p^{(i)}_{\text{accept}}.$$

4. Return sorted event times:

   The set of accepted event times $\{t_{\text{events}}\}$ constitutes a realization of the NHPP with the desired intensity function $\lambda(t)$.

Once the refurbishment events are simulated, we map these continuous event times to discrete years within the operating life. For each event, we assign a refurbishment fraction representing the proportion of the equipment that requires refurbishment. This fraction is sampled from a uniform distribution between 15% and 40%, reflecting variability in the extent of refurbishment needed:

$$\text{Refurbishment Fraction} \sim \text{Uniform}(0.15, 0.40).$$

These fractions are accumulated for each year, ensuring that the total refurbishment cost does not exceed 100% of the initial capital cost in any given year. This process generates a stochastic refurbishment schedule that realistically models maintenance expenses over time.

3.3.2 Integration with Monte Carlo Simulation

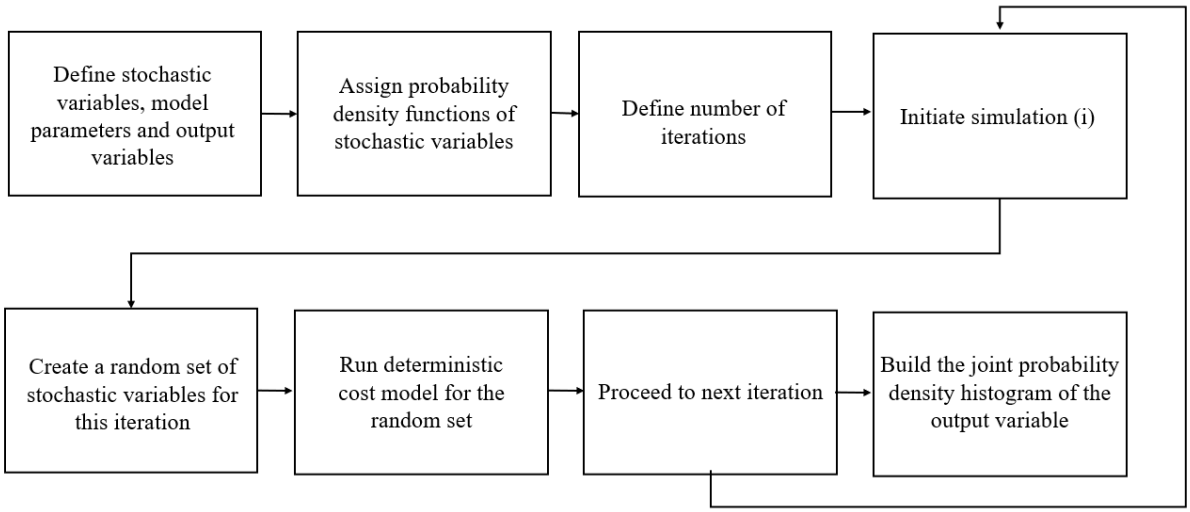

Figure 18: Workflow of the Monte Carlo simulation
Source: Adapted from Ioannou, Angus and Brennan (2017)

Integrating these stochastic refurbishment schedules into a Monte Carlo simulation framework allows us to assess their impact on the economic performance of the hydrogen production system. In each iteration of the simulation, we also sample other uncertain parameters influencing the system's economics, such as electricity cost and capacity factor.

These sampled parameters, along with the generated refurbishment schedule, are input into the ProFAST financial model. The model calculates the required commodity price (i.e., the price of hydrogen per kilogram) that results in a net present value (NPV) of zero, considering all cash flows over the project's life. By iterating this process numerous times (e.g., 1,000 simulations), we generate distributions of the commodity price and other economic indicators.

3.3.3 Evaluation

The evaluation of the simulation results will focus on the comprehensive analysis of the empirical distribution of the levelized cost of hydrogen (LCOH) for the two scenarios of electricity generation, grid electricity and wind power, as well as the two hydrogen production pathways,

water electrolysis and ammonia electrolysis.

The empirical distribution of the LCOH will be analyzed using statistical metrics and visualizations such as histograms and cumulative distribution functions (CDFs). These tools will allow for the identification of central tendencies (mean and median), variability (standard deviation), and the range of LCOH outcomes across 1,000 Monte Carlo simulation iterations for each scenario and pathway. Special attention will be given to the tails of the distributions to assess the risk of extreme outcomes, which is particularly relevant for evaluating the feasibility of hydrogen production under less favorable conditions.

Additionally, the composition of the LCOH will be examined by deconstructing the costs into their respective components through a net present value (NPV) analysis. This involves isolating and evaluating the contribution of individual cost elements, such as capital expenditures (CAPEX), operating expenditures (OPEX), feedstock costs, and refurbishment expenses, to the overall LCOH. By performing this decomposition, the analysis will reveal the relative importance of each cost driver and how it differs between the two electricity generation scenarios and the two hydrogen production methods

In conclusion, the evaluation framework provides a comprehensive and rigorous analysis of the economic performance of hydrogen production systems by integrating stochastic modeling of refurbishment events, electricity costs, and capacity factors into a Monte Carlo simulation. The comparative analysis of electricity generation methods and hydrogen production pathways further underscores the economic trade-offs and operational challenges associated with each approach.

4 RESULTS

4.1 Water electrolysis

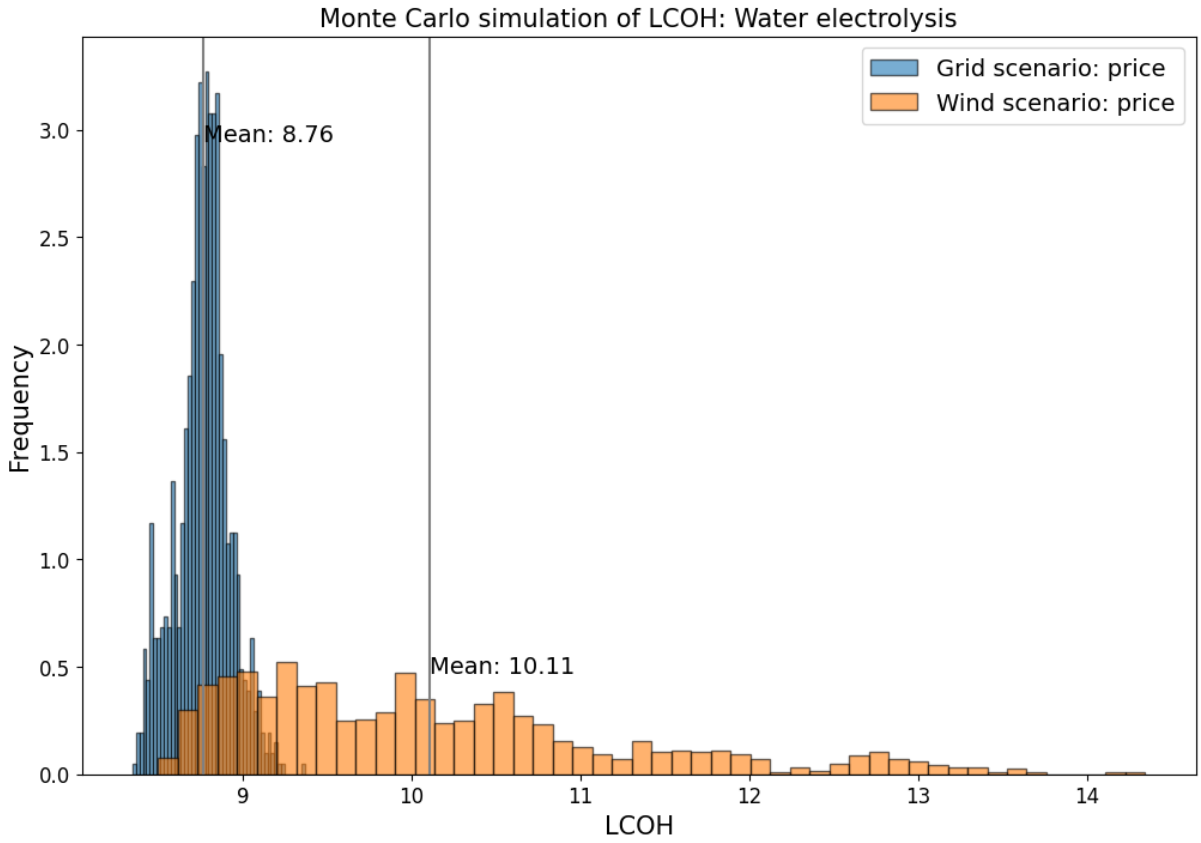

Figure 19: Histogram of simulated LCOH for water electrolysis
Source: Elaborated by the author

The Levelized Cost of Hydrogen (LCOH) results for water electrolysis exhibit very distinct statistical characteristics depending on the electricity source utilized, specifically grid or wind electricity. For the grid electricity scenario, the mean LCOH is reported at 8.76 USD/kg, with a standard deviation of 0.16 USD/kg. This low variability reflects the relative stability and predictability of grid electricity pricing and supply. In contrast, the wind electricity scenario

LCOH statistics (USD/kg)	**Water electrolysis**	
	Grid	Wind
Mean	8.76	10.11
Standard Deviation	0.16	1.15
Median	8.77	9.91
1% Value	8.41	8.63
99% Value	9.16	13.30

Table 6: Summary statistics for LCOH from water electrolysis
Source: Elaborated by the author

demonstrates a higher mean LCOH of 10.11 USD/kg, with a substantially greater standard deviation of 1.15 USD/kg, indicative of significant cost fluctuations driven by wind resource intermittency. .

The tails of the cost distribution provide additional insights. The 1% value for wind electricity is 8.63 USD/kg, showing that in optimal wind conditions, costs can approach grid-based scenarios. However, the upper end of the distribution, with a 99% value of 13.30 USD/kg, illustrates the impact of low wind availability on cost escalation. This discrepancy arises from the dependency of wind-based hydrogen production on capacity utilization. During periods of low wind availability, plant output decreases, leading to higher unit costs as fixed expenses are amortized over fewer hydrogen units.

A cost breakdown analysis (illustrated in figure 20) reveals that electricity costs, particularly the transmission tariff (TUSD) charges, are the most significant contributors to the LCOH in both scenarios. In the grid scenario, TUSD charges alone account for approximately 64% of the total mean cost, totaling 5.64 USD/kg. Although TUSD charges are reduced to 3.97 USD/kg in the wind scenario, the plant's lower utilization significantly amplifies the impact of fixed costs, including the PEM stack CAPEX and annual maintenance. These elements show considerably higher variability in the wind scenario, mirroring the volatility of wind availability.

The simulation of refurbishment events (showed in figure 21) had a low impact on the final Levelized Cost of Hydrogen (LCOH). This is shown from the standard deviation of the PEM stack's contribution in the grid scenario, which was 0.15USD/kg , representing only 2% of the total LCOH value.

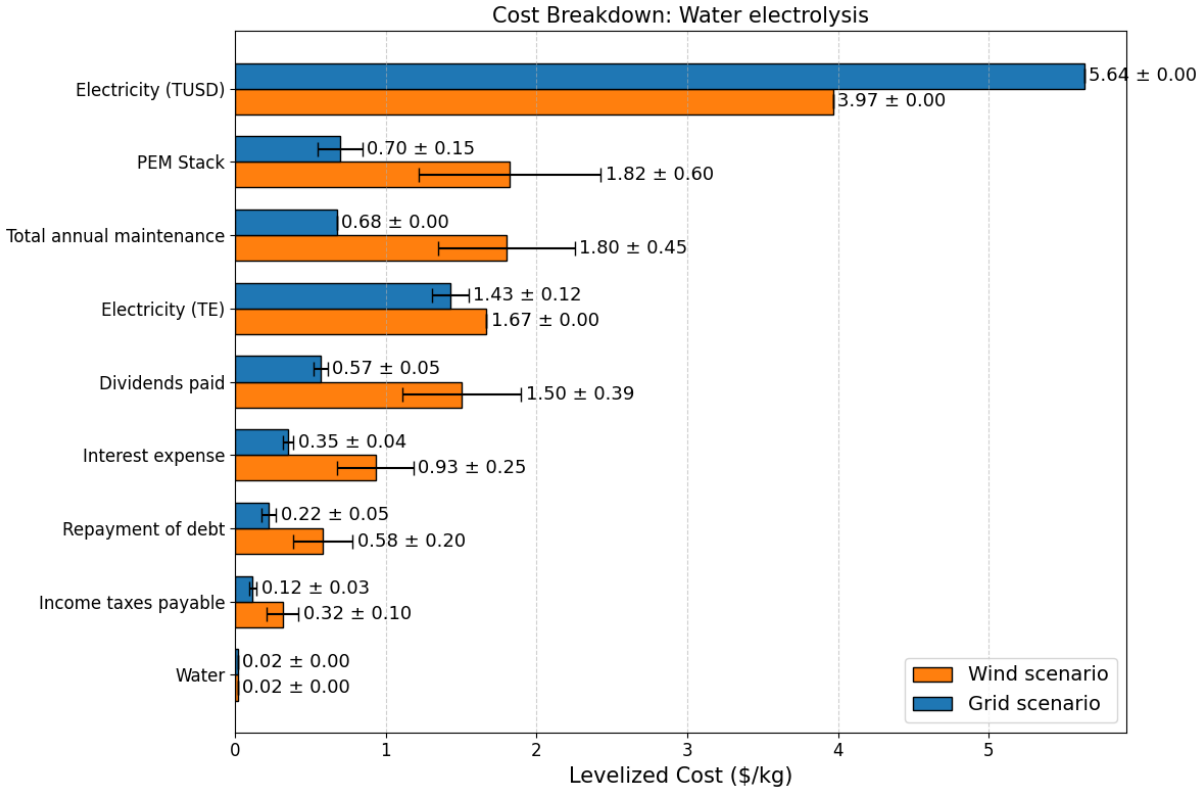

Figure 20: Breakdown of costs for water electrolysis
Source: Elaborated by the author

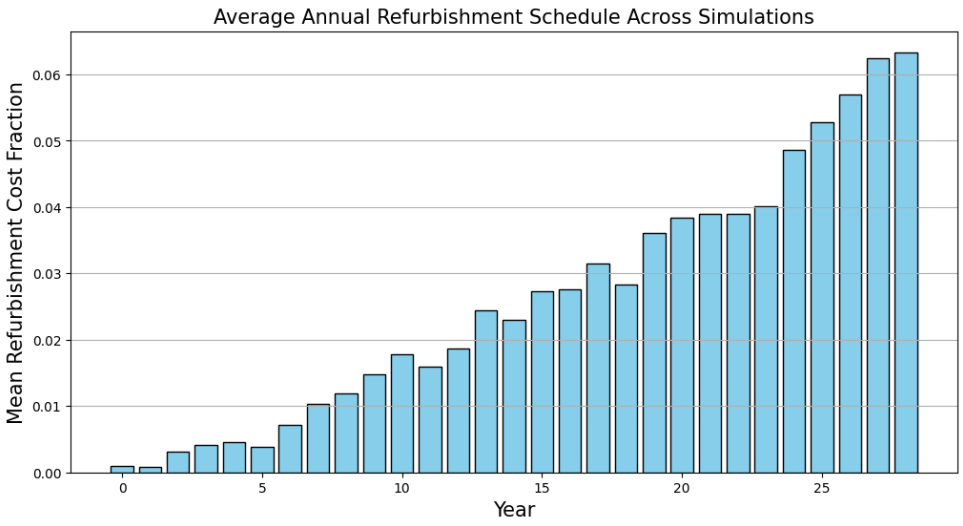

Figure 21: Mean CAPEX fraction resulting from the simulated refurbishment schedule
Source: Elaborated by the author

4.2 Ammonia electrolysis

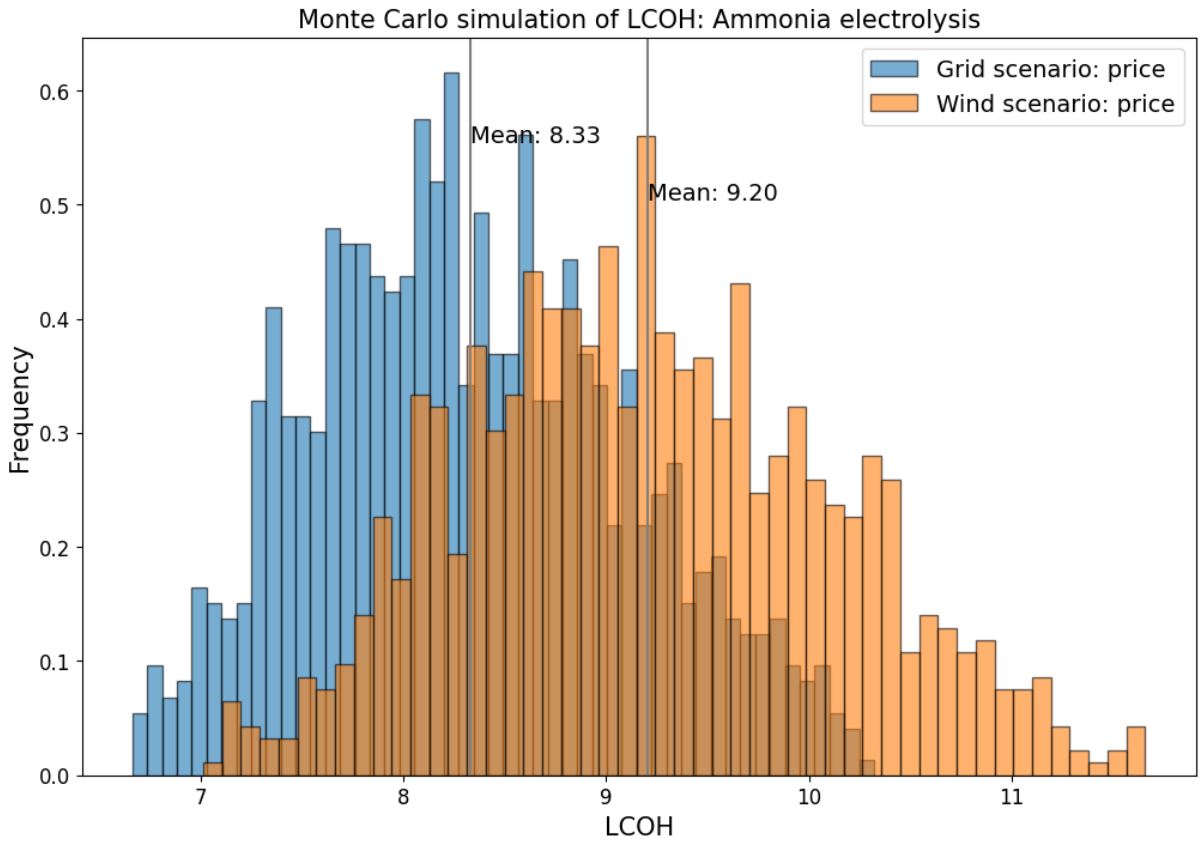

Figure 22: Histogram of simulated LCOH for ammonia electrolysis
Source: Elaborated by the author

LCOH statistics (USD/kg)	**Ammonia electrolysis**	
	Grid	Wind
Mean	8.33	9.2
Standard Deviation	0.77	0.9
Median	8.25	9.18
1% Value	6.81	7.25
99% Value	10.07	11.25

Table 7: Summary statistics for LCOH from ammonia electrolysis
Source: Elaborated by the author

Results for LCOH from ammonia electrolysis under both scenarios present a similar distribution, dominated by the triangular shape of the distribution assumed for the feedstock. Under the grid electricity scenario, mean LCOH was calculated at 8.33 USD/kg, with a median of 8.25 USD/kg. These closely aligned values suggest a symmetric distribution of costs, centered around the mean. In comparison, the wind electricity scenario yielded a higher mean LCOH of

9.2 USD/kg, with a median of 9.18 USD/kg, indicating a similar symmetry but at elevated cost levels. The higher mean for wind electricity reflects the additional expenses associated with variable capacity factors.

The standard deviation of the LCOH under the grid electricity scenario was 0.77 USD/kg, indicating moderate variability in cost outcomes. In contrast, the wind electricity scenario exhibited a higher standard deviation of 0.9 USD/kg, reflecting greater uncertainty and cost fluctuations due to variability in wind resource availability.

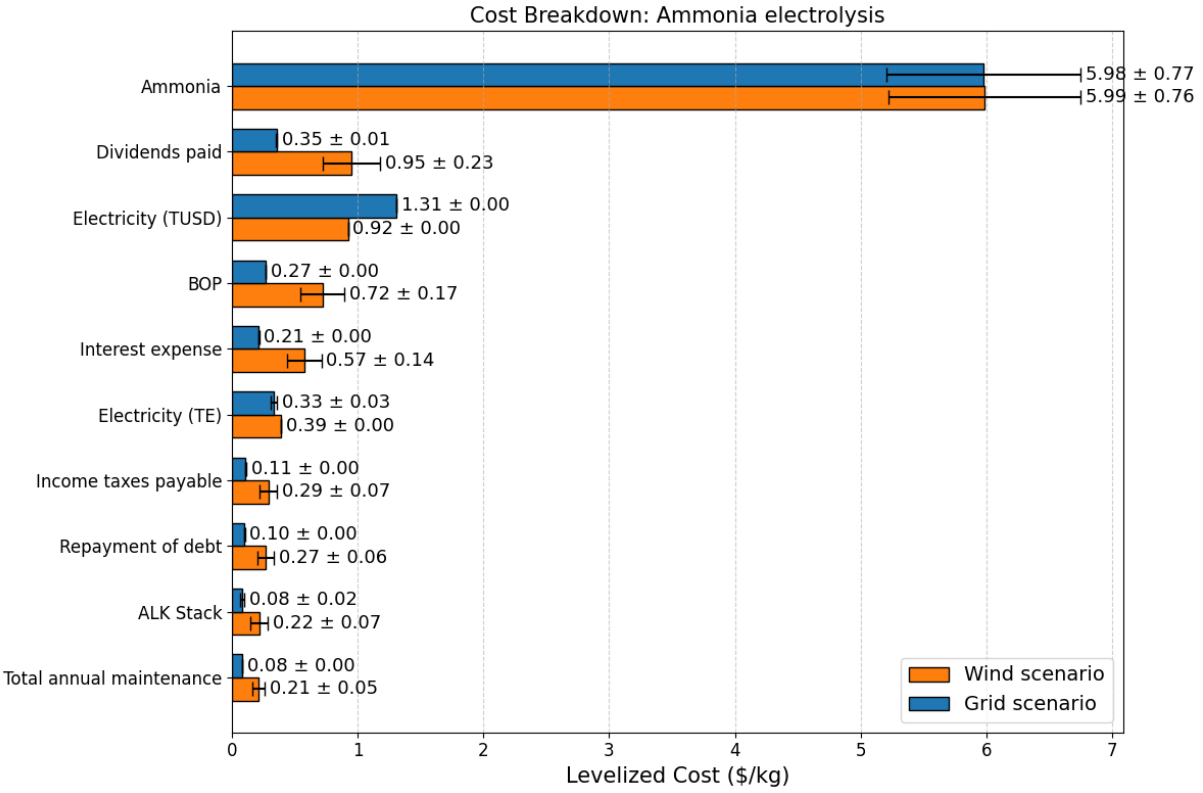

Figure 23: Breakdown of costs for ammonia electrolysis
Source: Elaborated by the author

Across both scenarios, the ammonia feedstock consistently emerges as the dominant cost driver, contributing the majority share to the total LCOH and being the largest source of cost variability. In the grid scenario, ammonia accounts for 5.98 USD/kg or 68.3% of the total mean cost. Similarly, in the wind scenario, ammonia represents 5.99 USD/kg or 54.8% of the total cost. This dominance highlights the critical importance of feedstock pricing in determining the economic feasibility of ammonia electrolysis.

Electricity costs, while less significant than feedstock costs, show clear differences between scenarios. In the grid scenario, combined electricity expenses total 1.64 USD/kg, with trans-

mission charges accounting for 1.31 USD/kg. By contrast, the wind scenario reduces electricity costs to 1.31 USD/kg but suffers from elevated fixed capital expenses. The alkaline (ALK) stack cost rises from 0.08 USD/kg in the grid scenario to 0.22 USD/kg in the wind scenario, while balance-of-plant (BOP) components increase from 0.27 USD/kg to 0.72 USD/kg. These increases reflect the impact of reduced utilization rates in the wind scenario, which amplify the per-unit burden of fixed costs

4.3 Comparative analysis

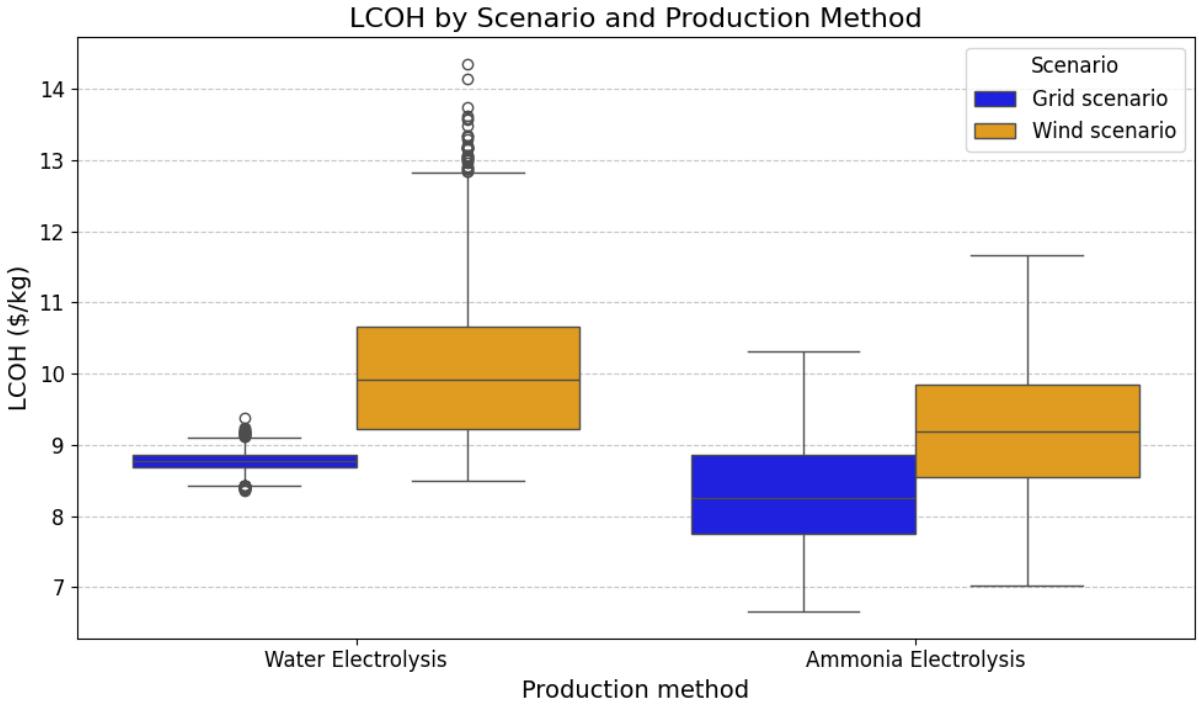

Figure 24: LCOH comparison across simulation scenarios

Source: Elaborated by the author

Water and ammonia electrolysis pathways exhibit distinct cost profiles under both grid and wind electricity scenarios. For the grid electricity scenario, water electrolysis has a higher mean LCOH of 8.76 USD/kg, compared to 8.33 USD/kg for ammonia electrolysis, but its values are much less dispersed, presenting a standard deviation of 0.16 versus 0.77 which resulted from the ammonia pathway. This difference is largely driven by the dominance of electricity costs in water electrolysis, which account for approximately 72.7% of total costs (including *TUSD* and *TE*), compared to 18.8% for ammonia electrolysis. In contrast, ammonia electrolysis relies heavily on feedstock costs, with ammonia alone constituting 68.3% of its total cost and bringing considerable influence to the result.

For the wind electricity scenario, both pathways produced dispersed results, although water electrolysis suffered more from the intermittency of wind. Water electrolysis also exhibits a higher mean LCOH of 10.11 USD/kg, compared to 9.20 USD/kg for ammonia electrolysis. The increased cost in water electrolysis stems from higher capital-related expenses, particularly for the PEM stack and maintenance. Ammonia electrolysis, while also experiencing elevated capital costs under wind electricity, benefits from its relatively lower reliance on electricity, which constitutes only 11.9% of its total cost compared to 50.9% for water electrolysis.

4.4 Discussion

The results from the simulation point towards ammonia is a practical hydrogen carrier, demonstrating its potential to compete with the conventional pathway of water electrolysis for hydrogen production in specific scenarios. This outcome is largely attributed to the high cost of electricity in Brazil, which significantly elevates the LCOH for the water electrolysis pathway. These findings support the proposition that green ammonia could be economically produced in regions with abundant renewable energy and low electricity costs and subsequently exported for reconversion into hydrogen in areas where renewable resources are less accessible.

When comparing the calculated LCOH values with established benchmarks, the results align with the higher end of reported estimates. For instance, a report by Lazard (2024) identifies a range of 4.45–6.05 USD/kg H2 for proton exchange membrane (PEM) water electrolysis in the United States. However, this range benefits from the lower electricity tariffs available in that country. Regarding ammonia, a recent study by Kanaan et al. (2023) reported an LCOH of 8.59 USD/kg H2 for large-scale electrolysis in Europe, a figure consistent with our findings, although their study did not include an analysis of the distribution of this result.

Meanwhile, McKinsey (2024) projected a LCOH range of 1.6–2.3 USD/kg H2 for water electrolysis in Brazil by 2030. However, these estimates are based on self-generation of renewable electricity, bypassing Brazil's high grid tariffs, which fundamentally distinguishes their model from ours. Nonetheless, the report aligns with our results in indicating a 10% cost reduction in cases where the plant leverages grid electricity, due to improved electrolyzer capacity and utilization.

Additionally, a critical consideration in relying on grid electricity in Brazil is the variability of the share of renewable energy in the final mix. During drought years, thermal power plants fueled by fossil energy are dispatched to preserve hydropower reservoirs, potentially lowering the renewable share below the 90% threshold required for green hydrogen certification. To

address this issue, a hybrid approach that combines grid electricity with renewable energy procured through power purchase agreements (PPAs) or self generated is advisable. This strategy ensures greater energy reliability, cost optimization, and adherence to renewable energy certification standards.

The elevated TUSD charges significantly increase the LCOH when using grid electricity. This finding underscores the potential impact of governmental subsidies or policy reforms in reducing grid charges. By alleviating these costs, policymakers can make green hydrogen production more economically competitive and attractive for investors. This fact also encourages self generation though dedicated infrastructure in order to prevent paying these tariffs.

Finally, the simulations revealed that equipment failures and associated refurbishment costs have a minimal impact on the overall LCOH. This finding suggests that concerns over electrolyzer lifespan and maintenance may be less critical than previously assumed, paving the way for more optimistic long-term planning and investment in hydrogen production facilities. This insight contributes to the growing confidence in the scalability and economic sustainability of hydrogen technologies.

5 CONCLUSION

This study developed and applied a failure simulation model to evaluate the Levelized Cost of Hydrogen (LCOH) across water and ammonia electrolysis pathways under grid and wind electricity scenarios. While the failure model was successfully implemented, it was found to have minimal impact on the overall LCOH. This result highlights the robustness of hydrogen production cost models to equipment failure, underscoring the importance of other cost drivers such as electricity pricing and feedstock costs.

The simulation model proved to be versatile and highly customizable, providing a valuable framework for analyzing different hydrogen production processes under stochastic conditions. This adaptability ensures that the model can be repurposed for future studies, broadening its applicability to other industrial processes characterized by variable inputs and uncertainties.

The findings also highlight ammonia electrolysis as a viable alternative for hydrogen production, particularly in contexts where electricity costs are high, as seen in Brazil. However, significant challenges remain, including the need to scale production and foster sufficient demand to justify large-scale investment. The economic feasibility of ammonia-based hydrogen production will depend on advances in technology, infrastructure, and market development.

This topic is quite rich and there is still much to be explored. For further studies, we suggest the devolopment of a scenario taking into consideration spot prices of renewable energy during the day, in order to optimize the operation of the electrolyzer by selling contracted electricity when there is too much of it, and buying from the grid when the production is low. Another potential area of research involves analyzing the profitability of hydrogen production using curtailed renewable energy, balancing the risk of plant idleness with the benefits of utilizing otherwise wasted electricity. Lastly, comparing the LCOH of ammonia conversion processes that that do not require electricity, such as thermal decomposition, could provide further insights into cost-effective hydrogen production methods.

REFERENCES

AGYEKUM, E. et al. A critical review of renewable hydrogen production methods: Factors affecting their scale-up and its role in future energy generation. *Energies*, v. 12, p. 173, 2022.

ALDERSEY-WILLIAMS, J.; RUBERT, T. Levelised cost of energy – a theoretical justification and critical assessment. *Energy Policy*, v. 124, p. 169–179, 2019. ISSN 0301-4215.

ANEEL. *Base Tarifária - Luz na Tarifa*. 2024. Accessed: 2024-11-17. Available on: <https://portalrelatorios.aneel.gov.br/luznatarifa/basestarifas>.

AZIZ, M. et al. Ammonia utilization technology for thermal power generation: A review. *Journal of the Energy Institute*, v. 111, p. 101365, 2023. ISSN 1743-9671. Available on: <https://www.sciencedirect.com/science/article/pii/S1743967123001940>.

AZIZ, M.; WIJAYANTA, A. T.; NANDIYANTO, A. B. D. Ammonia as effective hydrogen storage: A review on production, storage, and utilization. *Energies*, v. 13, n. 3062, 2020. Available on: <https://doi.org/10.3390/en13123062>.

BARROS, J. J. C. et al. Probabilistic life-cycle cost analysis for renewable and non-renewable power plants. *Energy*, v. 112, p. 774–787, 2016. ISSN 0360-5442. Available on: <https://www.sciencedirect.com/science/article/pii/S0360544216308726>.

BARTELS, J. R. *A feasibility study of implementing an Ammonia Economy*. : Iowa State University, 2008.

BAñARES-ALCáNTARA, R.; SALMON, N.; VALERA-MEDINA, A. Green ammonia as a spatial energy vector: A review. *Sustainable Energy & Fuels*, v. 5, p. 2814–2839, 2021. Available on: <https://doi.org/10.1039/d1se00345c>.

BELL, T.; TORRENTE-MURCIANO, L. H2 production via ammonia decomposition using non-noble metal catalysts: A review. *Topics in Catalysis*, v. 59, 09 2016.

C3S. *Copernicus: June 2024 Marks 12th Month of Global Temperature Reaching 1.5°C Above Pre-Industrial*. Reading, UK: , 2024. Available on: <https://climate.copernicus.eu/copernicus-june-2024-marks-12th-month-global-temperature-reaching-15degc-above-pre-industrial>.

CANO, Z. P. et al. Batteries and fuel cells for emerging electric vehicle markets. *Nature Energy*, v. 3, n. 4, p. 279–289, 2018. ISSN 2058-7546. Available on: <https://doi.org/10.1038/s41560-018-0108-1>.

CAVALIERE, P. Hydrogen storage. In: *Water Electrolysis for Hydrogen Production*. Springer, 2023. Discusses hydrogen storage challenges, including low volumetric energy density and storage methods such as 700 bar compression and cryogenic liquid storage at -253°C. Available on: <https://link.springer.com/chapter/10.1007/978-3-031-37780-8_16>.

CENTRAL BANK OF BRAZIL. *Exchange Rates - Daily Data*. 2024. Accessed: 2024-11-11, USD to BRL exchange rate: X.XX. Available on: <https://www.bcb.gov.br>.

CLEVELAND, C. *Fuel energy density: What is it and why is it important?* 2024. Accessed: 02-11-2024. Available on: <https://visualizingenergy.org/fuel-energy-density-what-is-it-and-why-is-it-important/>.

CLEVELAND, F. R. B. OF. *Inflation Expectations*. 2024. Accessed: 2024-11-10. Available on: <https://www.clevelandfed.org/indicators-and-data/inflation-expectations>.

CLIMATE CENTRAL. *Climate Change and the Escalation of Global Extreme Heat*. Princeton, NJ: , 2024. Available on: <https://www.climatecentral.org/report/climate-change-and-the-escalation-of-global-extreme-heat>.

DAMODARAN, A. *Country Risk Premiums*. 2024. Accessed: 2024-11-11. Available on: <https://pages.stern.nyu.edu/~adamodar/New_Home_Page/datafile/ctryprem.html>.

DAMODARAN, A. *Data Sets: Debt and Leverage Ratios*. 2024. <https://pages.stern.nyu.edu/~adamodar/New_Home_Page/datafile/dbtfund.htm>. Accessed: 2024-11-10. Available on: <https://pages.stern.nyu.edu/~adamodar/New_Home_Page/datafile/dbtfund.htm>.

DAVIDSON, D. Exnovating for a renewable energy transition. *Nature Energy*, v. 4, p. 1–3, 03 2019.

DCIDE. *Denergia Dashboard*. 2024. Accessed: 2024-11-17. Available on: <https://denergia.com.br/dashboard>.

DECC. *Electricity Generation Costs*. 2013. Accessed: 28-10-2024. Available on: <https://www.gov.uk/government/uploads/system/uploads/attachment_data/file/223940/DECC_Electricity_Generation_Costs_for_publication_-_24_07_13.pdf.>

DEKKING, F. et al. *A Modern Introduction to Probability and Statistics: Understanding Why and How*. Springer London, 2006. (Springer Texts in Statistics). ISBN 9781846281686. Available on: <https://books.google.com.br/books?id=TEcmHJX67coC>.

DINCER, I. et al. Ammonia. In: ____. *Ammonia Energy Technologies*. Cham: Springer International Publishing, 2022. p. 1–22. ISBN 978-3-031-13532-3. Available on: <https://doi.org/10.1007/978-3-031-13532-3_1>.

DUIJM, N. J.; MARKERT, F.; PAULSEN, J. L. *Safety assessment of ammonia as a transport fuel*. : Risø National Laboratory, 2005.

EHLIG-ECONOMIDES, C.; HATZIGNATIOU, D. G. Blue hydrogen economy - a new look at an old idea. In: *SPE Annual Technical Conference and Exhibition*. Dubai, UAE: Society of Petroleum Engineers, 2021.

EUROPEAN COMISSION. *Commission sets out rules for renewable hydrogen*. 2023. Accessed: 2024-11-05. Available on: <https://ec.europa.eu/commission/presscorner/detail/en/ip_23_594>.

FALCONE, P. M.; HIETE, M.; SAPIO, A. Hydrogen economy and sustainable development goals: Review and policy insights. *Current opinion in green and sustainable chemistry*, Elsevier, v. 31, p. 100506, 2021.

FARRELL, N. Policy design for green hydrogen. *Renewable and Sustainable Energy Reviews*, v. 178, p. 113216, 2023. ISSN 1364-0321. Available on: <https://www.sciencedirect.com/science/article/pii/S1364032123000722>.

FOUQUET, R. Historical energy transitions: Speed, prices and system transformation. *Energy Research Social Science*, v. 22, p. 7–12, 2016. ISSN 2214-6296. Available on: <https://www.sciencedirect.com/science/article/pii/S2214629616301979>.

GAONKAR, A. et al. An assessment of validity of the bathtub model hazard rate trends in electronics. *IEEE Access*, IEEE, v. 9, p. 10282–10290, 2021.

GERBONI, R. 11 - introduction to hydrogen transportation. In: GUPTA, R. B.; BASILE, A.; VEZIROğLU, T. N. (Ed.). *Compendium of Hydrogen Energy*. Woodhead Publishing, 2016, (Woodhead Publishing Series in Energy). p. 283–299. ISBN 978-1-78242-362-1. Available on: <https://www.sciencedirect.com/science/article/pii/B9781782423621000110>.

GONZALEZ-GARAY, A. et al. Hydrogen production and its applications to mobility. *Annual Review of Chemical and Biomolecular Engineering*, v. 13, p. 501–28, 2022.

GRAVER, B.; ZHANG, K.; RUTHERFORD, D. *CO_2 Emissions from Commercial Aviation, 2018*. 2019. The authors provide a thorough analysis of the role of freight and passenger aviation in aviation-related CO_2 emissions, including how these sectors are predicted to change in future years.

HALL, D.; PAVLENKO, N.; LUTSEY, N. *Beyond Road Vehicles: Survey of Zero-emission Technology Options Across the Transport Sector*. 2018.

HECK, N.; SMITH, C.; HITTINGER, E. A monte carlo approach to integrating uncertainty into the levelized cost of electricity. *The Electricity Journal*, v. 29, n. 3, p. 21–30, 2016. ISSN 1040-6190. Available on: <https://www.sciencedirect.com/science/article/pii/S1040619016300240>.

HOWARTH, R. W.; JACOBSON, M. Z. How green is blue hydrogen? *Energy Science & Engineering*, v. 9, n. 10, p. 1676–1687, 2021. Available on: <https://scijournals.onlinelibrary.wiley.com/doi/abs/10.1002/ese3.956>.

HUBERT, M. et al. *Clean Hydrogen Production Cost Scenarios with PEM Electrolyzer Technology*. 2024. Available on: <https://www.hydrogen.energy.gov/docs/hydrogenprogramlibraries/pdfs/24005-clean-hydrogen-production-cost-pem-electrolyzer.pdf?sfvrsn=8cb10889_1>.

HUNTER, C. et al. *Energy Storage Analysis*. 2020.

IEA. *Projected Costs of Generating Electricity*. 2020. Accessed: 28-10-2024. Available on: <https://www.iea.org/reports/projected-costs-of-generating-electricity-2020>.

IEA. *Ammonia Technology Roadmap*. Paris, 2021. Licence: CC BY 4.0. Available on: <https://www.iea.org/reports/ammonia-technology-roadmap>.

IEA. *Net Zero by 2050*. IEA, 2021. 224 p. Available on: <https://www.oecd-ilibrary.org/content/publication/c8328405-en>.

IEA. *CO2 Emissions in 2023*. Paris: IEA, 2024a. Licence: CC BY 4.0. Available on: <https://www.iea.org/reports/co2-emissions-in-2023>.

IEA. *Global Hydrogen Review 2024*. Paris: IEA, 2024b. Licence: CC BY 4.0. Available on: <https://www.iea.org/reports/global-hydrogen-review-2024>.

IEA. *World Energy Outlook 2024*. Paris: IEA, 2024c. Licence: CC BY 4.0 (report); CC BY NC SA 4.0 (Annex A). Available on: <https://www.iea.org/reports/world-energy-outlook-2024>.

IEA, C. et al. Technology roadmap low-carbon transition in the cement industry. *France/WBCSD, Geneva, Switzerland. IEA, Paris*, 2018.

INCER-VALVERDE, J. et al. "colors" of hydrogen: Definitions and carbon intensity. *Energy Conversion and Management*, v. 291, p. 117294, 2023. ISSN 0196-8904. Available on: <https://www.sciencedirect.com/science/article/pii/S0196890423006404>.

IOANNOU, A.; ANGUS, A.; BRENNAN, F. Stochastic prediction of offshore wind farm lcoe through an integrated cost model. *Energy Procedia*, v. 107, p. 383–389, 2017. ISSN 1876-6102. 3rd International Conference on Energy and Environment Research, ICEER 2016, 7-11 September 2016, Barcelona, Spain. Available on: <https://www.sciencedirect.com/science/article/pii/S1876610216317696>.

IPCC. Summary for policymakers. In: MASSON-DELMOTTE, V. et al. (Ed.). *Global Warming of 1.5°C. An IPCC Special Report on the impacts of global warming of 1.5°C above pre-industrial levels and related global greenhouse gas emission pathways, in the context of strengthening the global response to the threat of climate change, sustainable development, and efforts to eradicate poverty*. Cambridge, UK and New York, NY, USA: Cambridge University Press, 2018. p. 3–24.

IPCC. *Climate Change 2023: Synthesis Report. Summary for Policymakers*. Geneva, Switzerland: , 2023. Available on: <https://www.ipcc.ch/report/ar6/syr/downloads/report/IPCC_AR6_SYR_SPM.pdf>.

IRENA. *Shaping Sustainable International Hydrogen Value Chains*. Abu Dhabi, 2024.

IRENA, H. F. R. P. Technology outlook for the energy transition. *IRENA, Abu Dhabi*, 2018.

JOSKOW, P. L. Comparing the costs of intermittent and dispatchable electricity generating technologies. *The American Economic Review*, American Economic Association, v. 101, n. 3, p. 238–241, 2011. ISSN 00028282. Available on: <http://www.jstor.org/stable/29783746>.

KANAAN, R. et al. Economical assessment comparison for hydrogen reconversion from ammonia using thermal decomposition and electrolysis. *Renewable and Sustainable Energy Reviews*, v. 188, p. 113784, 2023. ISSN 1364-0321.

KAYFECI, M.; KEçEBAş, A.; BAYAT, M. Chapter 3 - hydrogen production. In: CALISE, F. et al. (Ed.). *Solar Hydrogen Production*. Academic Press, 2019. p. 45–83. ISBN 978-0-12-814853-2. Available on: <https://www.sciencedirect.com/science/article/pii/B9780128148532000035>.

KEE, J.; PENEV, M. M. *ProFAST (Production Financial Analysis Scenario Tool) [SWR-23-88]*. 2023. [Computer Software] <https://doi.org/10.11578/dc.20231211.1>. Available on: <https://doi.org/10.11578/dc.20231211.1>.

KOVAč, A.; PARANOS, M.; MARCIUš, D. Hydrogen in energy transition: A review. *International Journal of Hydrogen Energy*, v. 46, n. 16, p. 10016–10035, 2021. ISSN 0360-3199. Hydrogen and Fuel Cells. Available on: <https://www.sciencedirect.com/science/article/pii/S0360319920345079>.

KUN, F.; COSTA, M. F.; ANDRADE, J. S. Modeling creep rupture in disordered materials as a non-homogeneous poisson process. *Physical Review E*, American Physical Society, v. 88, n. 4, p. 042105, 2013.

KöNIG, D. H. et al. Simulation and evaluation of a process concept for the generation of synthetic fuel from co2 and h2. *Energy*, v. 91, p. 833–841, 2015. ISSN 0360-5442. Available on: <https://www.sciencedirect.com/science/article/pii/S0360544215011767>.

LAWLESS, J. F.; CROWDER, M. Models and estimation methods for repairable systems. *Technometrics*, Taylor & Francis, v. 37, n. 1, p. 1–10, 1995.

LAZARD. *LCOE+ 2024*. 2024. Accessed: 22-10-2024. Available on: <https://www.lazard.com/media/xemfey0k/lazards-lcoeplus-june-2024-_vf.pdf>.

LEAL, F. I.; REGO, E. E.; RIBEIRO, C. DE O. Levelized cost analysis of thermoelectric generation in brazil: A comparative economic and policy study with environmental implications. *Journal of Natural Gas Science and Engineering*, v. 44, p. 191–201, 2017. ISSN 1875-5100. Available on: <https://www.sciencedirect.com/science/article/pii/S1875510017301865>.

LEE, C.-Y.; AHN, J. Stochastic modeling of the levelized cost of electricity for solar pv. *Energies*, v. 13, n. 11, 2020. ISSN 1996-1073. Available on: <https://www.mdpi.com/1996-1073/13/11/3017>.

LEWIS, P. A. W.; SHEDLER, G. S. Simulation of nonhomogeneous poisson processes by thinning. *Naval Research Logistics Quarterly*, v. 26, n. 3, p. 403–413, 1979.

LUCHERONI, C.; MARI, C. Co2 volatility impact on energy portfolio choice: A fully stochastic lcoe theory analysis. *Applied Energy*, v. 190, p. 278–290, 2017. ISSN 0306-2619. Available on: <https://www.sciencedirect.com/science/article/pii/S0306261916319080>.

MA, N. et al. Large scale of green hydrogen storage: Opportunities and challenges. *International Journal of Hydrogen Energy*, v. 50, p. 379–396, 2024. ISSN 0360-3199. Available on: <https://www.sciencedirect.com/science/article/pii/S0360319923045883>.

MACFARLANE, D. R. et al. A roadmap to the ammonia economy. *Joule*, Elsevier, v. 4, n. 6, p. 1186–1205, 2020.

MCKINSEY. *Hidrogênio verde: Uma oportunidade de geração de riqueza com sustentabilidade para o Brasil e o mundo*. 2024. Accessed: 2024-11-20. Available on: <https://www.mckinsey.com/br/en/our-insights/hidrogenio-verde-uma-oportunidade-de-geracao-de-riqueza-com-sustentabilidade-para-o-brasil-e-o-mund

MELAINA, M.; ANTONIA, O.; PENEV, M. *Blending Hydrogen into Natural Gas Pipeline Networks: A Review of Key Issues*. 2013.

Ministry of Mines and Energy. *Fontes renováveis responderam por 93,1% da geração de energia elétrica em 2023*. 2023. Accessed: 2024-11-11. Available on: <https://www.gov.br/mme/pt-br/assuntos/noticias/fontes-renovaveis-responderam-por-93-1-da-geracao-de-energia-eletrica-em-2023>.

NREL. *Simple Levelized Cost of Energy (LCOE) Calculator Documentation*. 2018. Accessed: 28-10-2024. Available on: <https://www.nrel.gov/analysis/tech-lcoe-documentation.html>.

OLIVEIRA, A. M.; BESWICK, R. R.; YAN, Y. A green hydrogen economy for a renewable energy society. *Current Opinion in Chemical Engineering*, v. 33, p. 100701, 2021. ISSN 2211-3398. Available on: <https://www.sciencedirect.com/science/article/pii/S2211339821000332>.

ONS. *Geração e Fator de Capacidade Médios Mensais*. 2024. Acesso em: 17 nov. 2024. Available on: <https://www.ons.org.br/Paginas/resultados-da-operacao/historico-da-operacao/geracao-fator-capacidade-medios-mensais.aspx>.

OZATO, J. Y. et al. Offshore wind power generation: An economic analysis on the brazilian coast from the stochastic lcoe. *Ocean Coastal Management*, v. 244, p. 106835, 2023. ISSN 0964-5691. Available on: <https://www.sciencedirect.com/science/article/pii/S0964569123003605>.

PENEV, M. Techno-economic modelling with h2a and h2fast. 3 2020. Available on: <https://www.osti.gov/biblio/1604304>.

PRATT, R. M.; LUZI, F.; FREEBURG, E. D. W. Analysis of hydrogen as a transportation fuel fy17 report. 9 2017. Available on: <https://www.osti.gov/biblio/1419921>.

RASUL, M. et al. The future of hydrogen: Challenges on production, storage and applications. *Energy Conversion and Management*, v. 272, p. 116326, 2022. ISSN 0196-8904. Available on: <https://www.sciencedirect.com/science/article/pii/S0196890422011049>.

REICHELSTEIN, S.; SAHOO, A. Time of day pricing and the levelized cost of intermittent power generation. *Energy Economics*, v. 48, p. 97–108, 2015. ISSN 0140-9883. Available on: <https://www.sciencedirect.com/science/article/pii/S0140988314003211>.

REUTERS. *Horizonte Minerals contrata energia para projeto de níquel Araguaia com Casa dos Ventos*. 2022. Accessed: 2024-11-11. Available on: <https://economia.uol.com.br/noticias/reuters/2022/11/23/horizonte-minerals-contrata-energia-para-projeto-de-niquel-araguaia-com-casa-dos-ventos.htm>.

RITCHIE, H.; ROSADO, P.; ROSER, M. Energy production and consumption. *Our World in Data*, 2020. Https://ourworldindata.org/energy-production-consumption.

ROTH, I. F.; AMBS, L. L. Incorporating externalities into a full cost approach to electric power generation life-cycle costing. *Energy*, v. 29, n. 12, p. 2125–2144, 2004. ISSN 0360-5442. Efficiency, Costs, Optimization, Simulation and Environmental Impact of Energy Systems. Available on: <https://www.sciencedirect.com/science/article/pii/S0360544204000945>.

ROUWENHORST, K. H.; CASTELLANOS, G. *Innovation outlook: Renewable ammonia*. : Irena, 2022.

SHEN, W. et al. A comprehensive review of variable renewable energy levelized cost of electricity. *Renewable and Sustainable Energy Reviews*, v. 133, n. C, 2020.

SMIL, V. What we need to know about the pace of decarbonization. *Substantia*, v. 3, n. 2, p. 69–73, Nov. 2019. Available on: <https://riviste.fupress.net/index.php/subs/article/view/700>.

SMITH, C.; HILL, A. K.; TORRENTE-MURCIANO, L. Current and future role of haber–bosch ammonia in a carbon-free energy landscape. *Energy & Environmental Science*, Royal Society of Chemistry, v. 13, n. 2, p. 331–344, 2020.

SQUADRITO, G.; MAGGIO, G.; NICITA, A. The green hydrogen revolution. *Renewable Energy*, v. 216, p. 119041, 2023. ISSN 0960-1481. Available on: <https://www.sciencedirect.com/science/article/pii/S0960148123009552>.

TAZI, N.; SAFAEI, F.; HNAIEN, F. Assessment of the levelized cost of energy using a stochastic model. *Energy*, v. 238, p. 121776, 2022. ISSN 0360-5442. Available on: <https://www.sciencedirect.com/science/article/pii/S0360544221020247>.

TIMILSINA, G. R. *Demystifying the Costs of Electricity Generation Technologies*. 2020. Available on: <https://ideas.repec.org/p/wbk/wbrwps/9303.html>.

UECKERDT, F. et al. System lcoe: What are the costs of variable renewables? *Energy*, v. 63, p. 61 – 75, 2013.

U.S. Energy Information Administration. *International Energy Outlook 2019 (IEO 2019)*. 2019.

VALERA-MEDINA, A. et al. Ammonia for power. *Progress in Energy and Combustion Science*, v. 69, p. 63–102, 2018. ISSN 0360-1285. Available on: <https://www.sciencedirect.com/science/article/pii/S0360128517302320>.

YORK, R.; BELL, S. E. Energy transitions or additions?: Why a transition from fossil fuels requires more than the growth of renewable energy. *Energy Research Social Science*, v. 51, p. 40–43, 2019. ISSN 2214-6296. Available on: <https://www.sciencedirect.com/science/article/pii/S2214629618312246>.

ZAMFIRESCU, C.; DINCER, I. Using ammonia as a sustainable fuel. *Journal of Power Sources*, v. 185, n. 1, p. 459–465, 2008. ISSN 0378-7753. Available on: <https://www.sciencedirect.com/science/article/pii/S0378775308004461>.

APPENDIX A – SIMULATIONS CODE

```
from ProFAST import ProFAST
import numpy as np
import matplotlib.pyplot as plt
import pandas as pd

def lambda_func(t, beta=2.5, eta=20.0):
    """
    Weibull hazard function to model refurbishment rate.

    Parameters:
    - t: Time variable (array-like).
    - beta: Shape parameter.
    - eta: Scale parameter.

    Returns:
    -   (t): Intensity at time t.
    """
    t = np.maximum(t, 1e-5)  # Avoid division by zero
    return (beta / eta) * (t / eta)**(beta - 1)

def simulate_refurbishment_events(beta, eta, operating_life):
    """
    Simulate refurbishment events over [0, T] years using an NHPP with a
    ↪ Weibull hazard function.
    """
    # Calculate  _max
    t_values = np.linspace(0.01, operating_life, 1000)
    lambda_values = lambda_func(t_values,beta, eta)
    lambda_max = np.max(lambda_values)

    # NHPP thinning algorithm
    N = np.random.poisson(lambda_max * operating_life)
    t_candidate = np.random.uniform(0, operating_life, N)
    acceptance_prob = lambda_func(t_candidate) / lambda_max
```

```
    u = np.random.uniform(0, 1, N)
    t_accepted = t_candidate[u <= acceptance_prob]
    t_events = np.sort(t_accepted)

    # Create refurbishment schedule
    refurb_schedule = [0.0] * (operating_life - 1)  # Initialize with
       ↪ zeros for years 1 to operating_life - 1
    for event_time in t_events:
        year = int(np.floor(event_time)) #gets the year when the event
           ↪ happened
        # Map events to years 1 to (operating_life - 1)
        if 1 <= year < operating_life:
            # Draw a random refurbishment fraction between 15% and 40%
            refurb_fraction = np.random.uniform(0.15, 0.40)
            refurb_schedule[year - 1] += refurb_fraction  # Subtract 1
               ↪ because refurb_schedule starts at year 1

    # Ensure refurbishment cost does not exceed 100% of initial cost in
       ↪ any year
    refurb_schedule = [min(x, 1.0) for x in refurb_schedule]
    return refurb_schedule

def monte_carlo_simulation_with_cost_breakdown(profast_instance,
   ↪ capital_item, n_simulations=1000, beta=2.5, eta=20.0,ammonia=False
   ↪ ):
    """
    Perform Monte Carlo simulation to analyze the effect of varying
       ↪ parameters on commodity price and cost breakdown.

    Parameters:
    -----------
    profast_instance: ProFAST
        An initialized instance of the ProFAST class
    capital_item: str
        The name of the capital item to simulate refurbishment
    n_simulations: int
        Number of Monte Carlo iterations
    beta: float
        Shape parameter for refurbishment event simulation
    eta: float
        Scale parameter for refurbishment event simulation

    Returns:
```

```
    --------
    results: dict
        A dictionary containing simulated prices, cost breakdowns, and
            ↪ related data for each scenario
    """

    # Electricity cost and capacity factor distributions for the two
        ↪ scenarios
    electricity_cost_distribution_TE = {
        'Grid scenario': lambda: np.random.choice(grid_tariff_data),  #
            ↪ USD/kWh
        'Wind scenario': lambda: 0.029  # Fixed cost under PPA
    }
    electricity_cost_distribution_TUSD = {
        'Grid scenario': lambda: 0.098,  # USD/kWh
        'Wind scenario': lambda: 0.069  # Fixed cost under PPA
    }

    capacity_factor_distribution = {
        'Grid scenario': lambda: 0.97,
        'Wind scenario': lambda: np.random.choice(capacity_factors)
    }

    # Dictionary to store results
    results = {
        'Grid scenario': {
            'price': [],
            'refurb': [],
            'electricity_cost_TE': [],
            'electricity_cost_TUSD': [],
            'capacity_factor': [],
            'cost_breakdown': pd.DataFrame()
        },
        'Wind scenario': {
            'price': [],
            'refurb': [],
            'electricity_cost_TE': [],
            'electricity_cost_TUSD': [],
            'capacity_factor': [],
            'cost_breakdown': pd.DataFrame()
        }
    }
```

```
    # Loop over the two scenarios
    for scenario in results:

        for i in range(n_simulations):
            # Sample electricity cost and capacity factor
            electricity_cost_TE = electricity_cost_distribution_TE[
                ↪ scenario]()
            electricity_cost_TUSD = electricity_cost_distribution_TUSD[
                ↪ scenario]()
            capacity_factor = capacity_factor_distribution[scenario]()

            # Set parameters in the ProFAST instance
            profast_instance.edit_feedstock('Electricity (TE)', {'cost':
                ↪  electricity_cost_TE})
            profast_instance.edit_feedstock('Electricity (TUSD)', {'cost
                ↪ ': electricity_cost_TUSD})
            profast_instance.set_params('long term utilization',
                ↪ capacity_factor)
            if ammonia:
                profast_instance.edit_feedstock('Ammonia', {'cost': np.
                    ↪ random.triangular(0.740,1,1.4)})


            # Simulate refurbishment schedule
            refurb_schedule = simulate_refurbishment_events(beta, eta,
                ↪ int(profast_instance.vals['operating life']))
            profast_instance.edit_capital_item(capital_item, {'refurb':
                ↪ refurb_schedule})

            # Solve for the commodity price for NPV = 0
            result = profast_instance.solve_price(guess_value=4)  #
                ↪ Initial guess: $2/unit

            # Extract cost breakdown
            cost_breakdown = profast_instance.get_cost_breakdown()
            cost_breakdown = cost_breakdown.reset_index()
            cost_breakdown['Iteration'] = i


            # Append the transposed cost breakdown to the scenario-
                ↪ specific DataFrame
            results[scenario]['cost_breakdown'] = pd.concat(
```

```
                [results[scenario]['cost_breakdown'], cost_breakdown],
                    ↪ ignore_index=True
            )

            # Append results
            results[scenario]['price'].append(result['price'])
            results[scenario]['refurb'].append(refurb_schedule)
            results[scenario]['electricity_cost_TE'].append(
                ↪ electricity_cost_TE)
            results[scenario]['electricity_cost_TUSD'].append(
                ↪ electricity_cost_TUSD)
            results[scenario]['capacity_factor'].append(capacity_factor)



    return results
```